forests

MDPI

Article

Effects of Summer Drought on the Fine Root System of Five Broadleaf Tree Species along a Precipitation Gradient

Sebastian Fuchs [1,*], Dietrich Hertel [1], Bernhard Schuldt [2] and Christoph Leuschner [1]

[1] Plant Ecology, Albrecht von Haller Institute for Plant Sciences, University of Goettingen, Untere Karspüle 2, 37073 Goettingen, Germany; dhertel@gwdg.de (D.H.); cleusch@gwdg.de (C.L.)

[2] Ecophysiology and Vegetation Ecology, Julius-von-Sachs-Institute of Biological Sciences, University of Würzburg, Julius-von-Sachs-Platz 3, 97082 Würzburg, Germany; bernhard.schuldt@uni-wuerzburg.de

* Correspondence: sfuchs@gwdg.de; Tel.: +49-551-397084

Received: 21 January 2020; Accepted: 25 February 2020; Published: 3 March 2020

Abstract: While much research has addressed the aboveground response of trees to climate warming and related water shortage, not much is known about the drought sensitivity of the fine root system, in particular of mature trees. This study investigates the response of topsoil (0–10 cm) fine root biomass (FRB), necromass (FRN), and fine root morphology of five temperate broadleaf tree species (*Acer platanoides* L., *Carpinus betulus* L., *Fraxinus excelsior* L., *Quercus petraea* (Matt.) Liebl., *Tilia cordata* Mill.) to a reduction in water availability, combining a precipitation gradient study (nine study sites; mean annual precipitation (MAP): 920–530 mm year^{-1}) with the comparison of a moist period (average spring conditions) and an exceptionally dry period in the summer of the subsequent year. The extent of the root necromass/biomass (N/B) ratio increase was used as a measure of the species' belowground sensitivity to water deficits. We hypothesized that the N/B ratio increases with long-term (precipitation gradient) and short-term reductions (moist vs. dry period) of water availability, while FRB changes only a little. In four of the five species (exception: *A. platanoides*), FRB did not change with a reduction in MAP, whereas FRN and N/B ratio increased toward the dry sites under ample water supply (exception: *Q. petraea*). *Q. petraea* was also the only species not to reduce root tip frequency after summer drought. Different slopes of the N/B ratio-MAP relation similarly point at a lower belowground drought sensitivity of *Q. petraea* than of the other species. After summer drought, all species lost the MAP dependence of the N/B ratio. Thus, fine root mortality increased more at the moister than the drier sites, suggesting a generally lower belowground drought sensitivity of the drier stands. We conclude that the five species differ in their belowground drought response. *Q. petraea* follows the most conservative soil exploration strategy with a generally smaller FRB and more drought-tolerant fine roots, as it maintains relatively constant FRB, FRN, and morphology across spatial and temporal dimensions of soil water deficits.

Keywords: Acer platanoides; Carpinus betulus; fine root biomass; fine root necromass; Fraxinus excelsior; necromass/biomass ratio; Quercus petraea; root morphology; Tilia cordata; water availability

1. Introduction

Tree fine roots (roots < 2 mm in diameter) play a crucial role in forest ecosystem functioning, even though they represent only a few percent of tree biomass [1–3]. Fine roots serve as the interface between soil and tree and thus control water and nutrient uptake, they closely interact with mycorrhizal fungi and rhizosphere microbiota, and represent a major source of soil organic carbon (C) [4,5]. Due to their rapid turnover, it has been estimated that up to a third of the global annual net primary production

refers to fine root growth [2]. The size, morphology, and turnover rate of the fine root system of trees is dependent on many biotic and abiotic factors. Water availability is a key determinant among the soil factors besides nutrient availability, soil acidity, and temperature [6–9].

With climate change, forests are exposed to warmer summers and a higher evaporative demand, and, in various regions, reduced and more irregular summer precipitation [10,11], likely exposing trees to increased drought and heat stress. Recent reviews of climate change-related decreases in tree vitality and increasing mortality in many forest regions of the earth have predominantly focused on aboveground tree parts [12–15], ignoring root responses. This is primarily caused by the fact that the fine root system of mature forests is difficult to observe, and methods are labour-intensive and often quite imprecise [6].

How tree roots and the root system respond to drought is increasingly a matter of debate, but the empirical data basis is quite limited, especially for mature trees. Optimal partitioning theory (OPT) predicts that trees tend to increase their root-to-shoot ratio (R/S) under conditions of limited water availability to increase their absorptive capacity in relation to the transpiring surface [6,16,17]. Evidence in support of OPT has been obtained by comparing the R/S of different plant functional types from different biomes [18,19], by analysing the R/S of trees or forests along precipitation gradients [20,21], and by manipulating soil moisture in experiments with tree saplings [22–24]. Most studies with increases in R/S found a reduction in aboveground biomass (leaf mass or shoot mass), while fine root biomass (FRB) changed only a little, suggesting that shoot growth may respond more sensitively to drought than root growth [25]. Yet, it is not well understood how the fine root system of trees responds to a decrease in soil water availability, and existing findings are partly contradictory [6,26,27]. Many sapling studies found a decrease in FRB with decreasing soil moisture [28–31], but these responses can hardly be extrapolated to mature trees, and limited rooting space may sometimes have influenced the results. For mature stands, Leuschner and Hertel [8] found in a meta-analysis of studies from temperate broad-leaved forests no clear trend in FRB in dependence on precipitation. The results of multi-site field studies with a single tree species are inconsistent: Some authors reported a higher FRB at drier sites [20,26,32,33], others a higher biomass at moister sites [7,27,34,35]. The controversial results are partly explained by differences in species, in the steepness of the precipitation gradient, or in the severity and timing of drought events at the study sites. Moreover, different combinations of growth-related reductions in overall productivity, of shifts in aboveground/belowground carbohydrate partitioning, and of altered root lifespan may lead to opposing root/shoot ratio responses [36].

More consistent are the reports about a fine root necromass (FRN) increase or elevated necromass/biomass (N/B) ratios as a consequence of drought exposure [6,37], indicating increased fine root mortality. In accordance, Hertel and Leuschner [38] found a large FRN increase in a mature beech forest after a summer drought, while FRB remained constant over the study period. It appears that certain tree species are capable of compensating elevated drought-induced fine root losses through increased production of new fine roots, thereby avoiding reductions in standing FRB. It is not known which species are capable of this response and under which conditions it occurs.

Root mortality reduces the lifespan of fine roots and, when dying roots are replaced by new ones, a reduction in mean fine root age in the root population is the consequence [36,39]. One possible physiological explanation of a shortened fine root lifespan in dry soil is active root shedding, in which fine roots act as 'hydraulic fuses' in the tree's xylem system, uncoupling the rest of the hydraulic system from low water potentials in the dry soil to avoid embolism formation in more expensive or irreplaceable plant organs [40–42]. This could happen when fine roots are indeed more sensitive to cavitation in the xylem than the stem and branches in the canopy. An alternative explanation assumes that younger fine roots, that replace the shed ones, are physiologically more active and therefore can support the tree by extracting more water, which increases fitness [6,39]. Such a response would also be in agreement with OPT, which predicts a higher investment in the root system. In any case, root mortality will increase the N/B ratio, which must be seen as an integral over the processes of root mortality and the production of new fine roots during the observation period, thus reflecting both

the root system's resistance to drought and its resilience after drought. The ratio has therefore been used in several studies and reviews as an indicator of tree and root system vitality under exposure to drought and chemical stress [7,37,43,44].

Field studies on the drought response of tree fine root systems usually adopt one of two approaches, either investigating temporal (natural or experimental) variation in soil moisture [45–50], or examining spatial differences in water availability, often along precipitation or soil moisture gradients [7,26,27,32,35,38,43,51]. In central Europe, such studies focused on the economically most important coniferous and broad-leaved tree genera, i.e., *Picea*, *Pinus*, *Fagus*, and *Quercus*.

Only little is known about the fine root system of other common tree species that are minor timber species or of no use in current forestry. Small-leaved lime (*Tilia cordata* Mill.), Norway maple (*Acer platanoides* L.), European hornbeam (*Carpinus betulus* L.), and European ash (*Fraxinus excelsior* L.) may be more drought resistant than European beech and Norway spruce according to their distribution ranges and knowledge of aboveground physiological traits [1,52]. While these species can be of interest for forestry in a warmer and drier climate in the future, their belowground drought response is unknown. Recent root research in temperate mixed forests with lime, maple, hornbeam, oak, and ash species has focused on species interactions and diversity effects, but drought responses have not been examined [53–55]. A better understanding of the belowground drought response of these minor timber species is fundamental for predicting the species' performance in a drier climate.

This study investigates the response of the fine root biomass and necromass, and fine root morphology of four secondary tree species (*T. cordata*, *A. platanoides*, *C. betulus*, and *F. excelsior*) to a reduction in water availability, combining a precipitation gradient study with the comparison of a moist and a dry season. The well-studied and relatively drought-resistant sessile oak (*Quercus petraea* (Matt.) Liebl.) was included in the study for comparison. The sample thus comprised three ECM (ectomycorrhizal; *T. cordata*, *C. betulus*, *Q. petraea*) and two AM tree species (arbuscular mycorrhizal; *A. platanoides*, *F. excelsior*), and two ring-porous (*Q. petraea*, *F. excelsior*) and three diffuse-porous species (*T. cordata*, *C. betulus*, *A. platanoides*), thereby covering a broad range of tree functional types of the European temperate tree flora. Fine root inventories were carried out in the topsoil of nine study sites along a precipitation gradient (mean annual precipitation (MAP): 918–528 mm year^{-1}), comparing data from a moist (spring 2017) and a subsequent dry period (summer 2018). The precipitation gradient covers most of the MAP range encountered by the species at their natural occurrences in northern central Europe.

We expected that the five species differ in their root system response to water deficits and that the sensitivity of belowground and aboveground organs are linked to each other in these species. The extent of the N/B ratio increase was used as a measure of the species' belowground sensitivity to water deficits. Based on the existing knowledge about the drought response of tree fine root systems [6,26,27], we hypothesized that, in all species, (i), the fine root N/B ratio increases with decreasing mean annual precipitation due to higher root mortality and thus an increase in necromass, while biomass changes only little, (ii) a severe summer drought increases necromass and the N/B ratio, and (iii) the increase in the N/B ratio upon drought is more pronounced at the moister sites, where trees are assumed to be more sensitive to water shortage.

2. Materials and Methods

2.1. Site Description

2.1.1. Forest Stands and Tree Species

Nine study sites were chosen along a transect in central Germany between Göttingen and Halle/S., which represents a steep precipitation gradient in west-east orientation. All sites are in the planar to colline zone (110–440 m a.s.l.) and have a cool-temperate climate with annual mean temperatures of 7.9 to 9.9 °C. Mean annual precipitation (MAP) ranges between 918 and 528 mm and mean growing

season precipitation (MGSP, April–September) between 291 and 412 mm, with a general decrease from west to east (Figure 1).

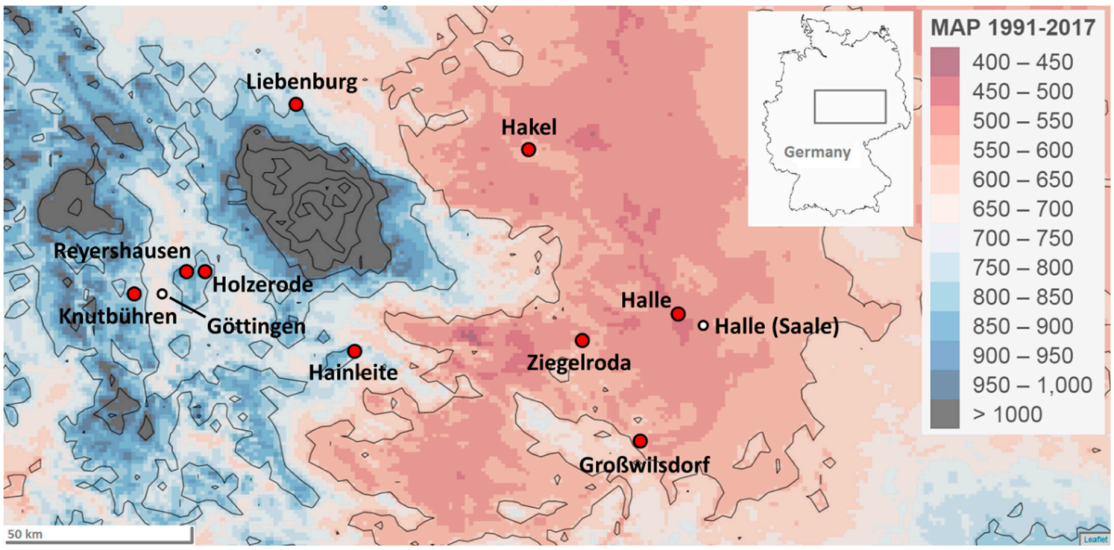

Figure 1. Map of the study area between Göttingen and Halle/S. in central Germany with the precipitation gradient from the west to the east. The nine study sites are marked with red dots. The colors indicate the mean annual precipitation (MAP 1991–2017). The area with MAP over 1000 mm NE of Göttingen is the Harz mountain range.

Four of the five investigated tree species (*A. platanoides*, *T. cordata*, *C. betulus*, and *F. excelsior*) are widespread in Central Europe with natural occurrences in various types of broadleaf mixed forest communities of the phytosociological alliances Carpinion betuli (oak-hornbeam forests) and Tilio-Acerion (mixed maple slope forests), in which European beech (*Fagus sylvatica* L.), the dominant species of Central Europe's natural forest vegetation, is rare or absent [1]. The four species are more demanding in terms of soil base saturation than beech and *Q. petraea*, the fifth species of this study, but they also occur in eastern Europe under a more continental climate and thus are thought to be relatively drought tolerant. While *Q. petraea* is one of the most important timber species of Central European forestry, the four other species are only secondary timber species in the study region. Therefore, mixed stands of comparable stand structure and tree age with presence of all five species are uncommon. As a consequence, not all species are present at all nine study sites, but every species occurs at least at five sites along the precipitation transect. Every site consisted of several mixed forests of variable species composition in a maximum distance of several hundred m to a few km to each other. The target species grew in these mixed stands of two to six species under comparable edaphic and climatic conditions. All stands were located on level terrain with an inclination of less than 5° without groundwater influence.

The target trees in the stands were all of mature age (range: 69–139 years), with the exception of two older oak stands (170 years). The exact age of all individuals was determined from the investigation of increment cores and dendrochronological analysis, except for *C. betulus*, which was not included in the tree ring study, as the increment cores consist of long sections of indistinguishable annual rings. Age information for this species was taken from forest inventory data supplied by the local forestry offices. The investigated trees were selected for comparable height and DBH at the different sites (Table 1). From the moister western to the drier eastern sites, average tree height in the stands slightly decreased from 28.2 to 25.8 m (means of all species), while average DBH increased from 44.5 to 47.1 cm. This indicates that aboveground biomass changes only little along the transect. Only in the case of *T. cordata*, tree height decreased notably towards the drier sites. In case of *F. excelsior*, we selected only trees that were not visibly affected by ash dieback, a recently spreading lethal infection caused by the fungus *Chalara fraxinea*.

Table 1. Site and tree characteristics of the nine study sites with the each 2–5 species occurring in the stands, sorted in ascending order of mean annual precipitation (MAP).

Site	Species	Lati-Tude	Longi-Tude	Altitude (m a.s.l.)	Mean Tree Age [1]	Mean Tree Height (m)	DBH (cm)	MAP (mm)	MGSP (mm)	MAT (°C)	pH (H_2O)	C/N Ratio	Soil Texture
Halle	*Acer platanoides*	51.49	11.89	135	69	24.6	40.9	527.8	291.1	9.94	6.11	15.32	loamy sand
Halle	*Quercus petraea*	51.49	11.87	134	167	24.7	55.3	530.8	293.2	9.84	4.35	15.21	loam
Halle	*Tilia cordata*	51.49	11.87	134	102	23.4	47.5	530.8	293.2	9.84	4.35	15.21	loam
Halle	*Carpinus betulus*	51.50	11.93	110	80	25.7	39.7	532.9	294.3	9.94	4.96	18.89	loam
Halle	*Fraxinus excelsior*	51.50	11.93	110	71	28.5	47.3	532.9	294.3	9.94	4.96	18.89	loam
Ziegelroda	*Fraxinus excelsior*	51.43	11.53	224	118	28.9	49.6	560.5	299.6	9.30	4.91	13.17	silt
Ziegelroda	*Tilia cordata*	51.43	11.53	224	136	25.7	51.5	560.5	299.6	9.30	4.91	13.17	silt
Ziegelroda	*Carpinus betulus*	51.43	11.52	263	116	27.0	47.5	583.8	307.2	9.13	4.24	15.67	silt
Ziegelroda	*Quercus petraea*	51.43	11.52	263	116	28.5	50.5	583.8	307.2	9.13	4.24	15.67	silt
Hakel	*Acer platanoides*	51.88	11.32	239	97	24.3	40.0	606.5	316.7	9.18	6.21	10.69	silt
Hakel	*Carpinus betulus*	51.88	11.32	239	133	23.8	45.3	606.5	316.7	9.18	6.21	10.69	silt
Hakel	*Fraxinus excelsior*	51.88	11.32	239	104	28.0	45.8	606.5	316.7	9.18	6.21	10.69	silt
Hakel	*Quercus petraea*	51.88	11.32	239	172	28.9	56.1	606.5	316.7	9.18	6.21	10.69	silt
Hakel	*Tilia cordata*	51.88	11.32	239	138	27.5	50.2	606.5	316.7	9.18	6.21	10.69	silt
Großwilsdorf	*Carpinus betulus*	51.19	11.75	243	133	22.9	44.6	624.6	327.0	9.30	4.67	14.06	silty loam
Großwilsdorf	*Fraxinus excelsior*	51.18	11.77	202	70	27.0	39.6	624.6	327.0	9.30	6.25	15.50	clay loam
Großwilsdorf	*Quercus petraea*	51.19	11.75	243	139	25.7	47.9	624.6	327.0	9.30	4.67	14.06	silty loam
Großwilsdorf	*Tilia cordata*	51.19	11.75	243	100	24.4	40.7	624.6	327.0	9.30	4.67	14.06	silty loam
Liebenburg	*Carpinus betulus*	52.02	10.42	186	98	29.1	44.6	708.3	341.4	9.51	6.34	11.70	silt
Reyershausen	*Tilia cordata*	51.60	10.01	276	114	31.5	50.6	768.9	359.5	8.93	6.46	12.00	silty clay loam
Knutbühren	*Acer platanoides*	51.54	9.81	319	90	24.8	40.4	780.2	354.3	8.60	n.a.	n.a.	silty loam
Knutbühren	*Carpinus betulus*	51.54	9.81	319	95	24.8	41.7	780.2	354.3	8.60	n.a.	n.a.	silty loam
Knutbühren	*Fraxinus excelsior*	51.54	9.81	319	98	26.7	47.9	780.2	354.3	8.60	n.a.	n.a.	silty loam
Holzerode	*Carpinus betulus*	51.59	10.08	268	112	26.8	42.9	812.8	376.1	8.80	4.71	15.44	sandy loam
Holzerode	*Quercus petraea*	51.59	10.08	268	114	27.6	53.3	812.8	376.1	8.80	4.71	15.44	sandy loam
Liebenburg	*Quercus petraea*	51.98	10.44	253	119	30.6	55.3	828.7	380.6	9.01	5.59	12.98	silty clay loam
Liebenburg	*Acer platanoides*	51.98	10.43	285	120	27.4	47.9	831.1	382.3	8.99	5.02	12.63	silt loam
Liebenburg	*Fraxinus excelsior*	51.98	10.43	285	111	30.9	52.0	831.1	382.3	8.99	5.02	12.63	silt loam
Hainleite	*Acer platanoides*	51.40	10.66	442	130	27.5	45.3	838.6	363.9	7.94	4.96	15.38	silt loam
Hainleite	*Carpinus betulus*	51.40	10.66	442	105	21.7	40.5	838.6	363.9	7.94	4.96	15.38	silt loam
Hainleite	*Fraxinus excelsior*	51.40	10.66	442	113	29.1	50.1	838.6	363.9	7.94	4.96	15.38	silt loam
Hainleite	*Quercus petraea*	51.40	10.66	442	93	22.4	36.8	838.6	363.9	7.94	4.96	15.38	silt loam
Reyershausen	*Acer platanoides*	51.59	10.01	398	109	28.6	38.3	917.8	412.1	8.17	6.01	12.27	silty clay loam
Reyershausen	*Fraxinus excelsior*	51.59	10.01	398	109	32.1	43.9	917.8	412.1	8.17	6.01	12.27	silty clay loam

[1] Mean tree age for all species except *C. betulus* was determined from increment cores of all sampled trees and dendrochronological analysis. *C. betulus* stand age was taken from forest inventory data from the accountable forestry offices. No soil chemistry data is available for the site Knutbühren. DBH = Stem diameter at breast height; MAP = mean annual precipitation (period 1991–2017); MGSP = mean growing season precipitation (April–September); MAT = mean annual temperature; soil texture is defined according to the nomenclature of the FAO (Food and Agriculture Organization of the United Nations).

2.1.2. Climatic Conditions

Precipitation, air temperature, and potential evapotranspiration (PET) data were taken from the DWD (Deutscher Wetterdienst, Offenbach, Germany) database and the required local data were calculated from extrapolated 1 km-gridded data. The gridding method of the DWD employs the reduction to a reference elevation level, the calculation of inverse squared-distance weights (horizontal interpolation), and finally the transformation to the actual elevation of the grid point using regression over elevation [56,57]. This gridding method is relatively simple, but comparison and verification against other GIS-based interpolation methods [58] have confirmed its accuracy, which is partly a consequence of the relatively high weather station density in Germany. The largest distance between a study site and the closest weather station was ca. 7.1 km.

PET was extrapolated from data derived from the agrometeorological model AMBAV ("Agrarmeteorologisches Modell zur Berechnung der aktuellen Verdunstung", [59]) that is based on the Penman-Monteith equation. Without doubt, these agrometeorological PET data do not characterize potential forest evapotranspiration exactly, but the values are used in the study only for characterizing the weather conditions prior to the two fine root inventory campaigns.

The mean de Martonne Index (DMI) for the respective three-month periods prior to each sampling date was calculated by dividing precipitation sums by the mean temperature + 10 [60].

Long-term mean annual climate data were calculated for the period 1991–2017, because PET data generated with the AMBAV model are only available from DWD stations since 1991. Fine root data were modelled in dependence on a variety of parameters characterizing site water availability, notably mean annual precipitation (MAP), mean growing season precipitation (MGSP; April–September), and the climatic water balance (precipitation—PET, whole year and growing season). Because the ratio of summer precipitation to annual precipitation is constant and temperature is inversely proportional to precipitation along the transect, we obtained similar results for all tested variables in the correlation analyses and thus used in the analyses MAP as a proxy for climatic aridity along the transect. The actual precipitation in the 12 months prior to sampling was tested as well and resulted in the same patterns of correlation, as it was mostly proportional to MAP along the transect (see Appendix A Table A1 and Figure A1).

2.1.3. Edaphic Conditions

Various soil chemical and physical properties were analysed for the topsoil (0–10 cm of mineral soil) of three soil pits per site, notably soil texture, organic matter content, soil pH (in H_2O and in KCl), and organic C, organic N, and resin-extractable P content. Organic carbon and nitrogen concentrations were determined by gas chromatography (C/N elemental analysis) and the resin-extractable P concentration was determined with ICP-OES (inductively coupled plasma optical emission spectrometry) analysis, after P extraction with water using an anion-exchange resin and subsequent re-exchange of P with NaCl and NaOH solutions. The soil organic matter content was additionally determined through the dry ignition method at 600 °C, the soil texture by sieving (sand fractions) and sedimentation (silt fractions) according to the international standard ISO 11277.

2.2. Fine Root Inventories

2.2.1. Sampling Periods

To examine the effect of seasonal drought on fine root mortality, two inventories with determination of fine root biomass and necromass were carried out at all sites in spring 2017 and summer 2018. The first inventory in April 2017 was conducted after a moderately moist spring period in order to examine fine root mass under ample soil moisture conditions along the precipitation gradient without the influence of unusual drought periods. On the other hand, no soil frost was influencing this inventory, as the winter was mild with no harsh frost periods. A second inventory was conducted in September 2018 after an exceptionally dry summer with an extended rainless period to investigate the effect of pronounced soil drought on the fine root system. The summer of 2018 with its extraordinary heatwave

was on average 2.0–2.3 °C warmer and had 55–74% lower rainfall amounts than the average (1991–2017) in the study region. All study sites were exposed to very low rainfall between May and September prior to the inventory, with mostly <30 mm of precipitation per month (Table 2). We decided to report the average weather in the 3 months prior to each sampling date and related it to the long-term means of the respective seasons. A period length of three months was chosen, because loamy soils in the study region are known to desiccate only with some delay after precipitation ceased in a dry period, and the peak of fine root mortality thus typically happens after an additional time lag of 1–2 months, according to a root study in central northern Germany [38].

Table 2. PET, precipitation, and temperature in the three months prior to the sampling dates in 2017 and 2018. Given are the totals of potential evapotranspiration (PET) and precipitation (P), the deviation of P from the long-term mean (1991–2017) in percent, and the absolute deviation of the average temperature of the three-month period from the long-term mean (1991–2017) in that period in °C.

Site	2017				2018			
	PET (mm)	P (mm)	P Deviation (%)	T Deviation (°C)	PET (mm)	P (mm)	P Deviation (%)	T Deviation (°C)
Halle	45.9	78.4	−24.9	+0.02	405.2	78.9	−68.3	+2.14
Ziegelroda	44.5	86.0	−25.4	+0.04	396.6	78.0	−70.2	+2.26
Hakel	43.9	101.0	−19.3	+0.18	390.4	120.0	−55.2	+2.12
Großwilsdorf	46.6	93.0	−26.7	+0.08	396.5	93.3	−67.4	+2.17
Knutbühren	45.2	144.0	−24.4	+0.02	374.7	82.7	−73.0	+2.14
Holzerode	46.1	147.0	−24.4	+0.06	380.2	120.0	−62.9	+2.15
Liebenburg	48.1	127.0	−36.3	+0.38	384.6	101.0	−67.9	+2.06
Hainleite	40.2	177.0	−16.8	+0.17	374.0	80.0	−73.9	+2.08
Reyershausen	44.0	159.0	−25.1	+0.04	372.6	125.0	−62.9	+2.13

2.2.2. Fine Root Biomass and Necromass

Five mature, similarly-sized and vital trees were chosen per site and species, and two topsoil samples per tree extracted in 1.5 m distance from the stem base in eastern and western direction using a soil corer of 3.5 cm in diameter. These two samples were later combined to one, as we did not intend to study FRB variation within the same tree. For reasons of comparability, the second sampling campaign was conducted at coring locations in close vicinity of the previous campaign, but in a distance of 40 cm to exclude possible interference from the soil disturbance of the earlier coring.

Because the study focus was on the comparison of five species at many sites with a large number of samples, we had to restrict the sampling to the uppermost 10 cm of mineral soil (A-horizon), where drought effects are assumed to be largest. At all sites, the A-horizon contained by far the highest density of fine roots which decreased exponentially with soil depth. Organic layers on top of the soil were generally thin, consisted mainly of undecomposed litter and rarely contained fine roots.

The soil samples were transferred to plastic bags and stored at 4 °C in the laboratory until processing within 3 months. Prior to the root extraction procedure, the samples were soaked in tap water and carefully cleaned from attached soil residues under gently running water over a sieve of 0.25 mm mesh size. Only fine root fragments (<2 mm in diameter, >10 mm in length) of the target species were considered for analysis. In most samples, shrub and herb roots were rare or missing and the percentage of roots of non-target species was very small, because all sampling locations were situated in small monospecific forest patches of 5–10 individuals of the target species. The sorting of fine roots by species was done by morphological criteria (colour and surface structure of the root periderm, branching patterns of the rootlets, morphology of ectomycorrhizae in the ECM species), established in our lab during earlier work in mixed broadleaf forests in Central Germany [53–55]. Living (biomass) and dead roots (necromass) were distinguished under the stereomicroscope by inspecting colour, root elasticity, and cohesion of the cortex, periderm, and stele [38,61]. The fine root biomass and necromass of every sample was dried at 70 °C for 48 h and weighed and expressed as g L^{-1} soil volume.

We did not take any dead root particles <10 mm length into account, although this finest fraction of decaying root particles is known to represent a considerable portion of total FRN [7,62]. One reason

is the sheer impossibility to assign these particles to different tree species in samples containing more than one tree species. In addition, a main study aim was the analysis of the effect of the 2018 summer drought on the N/B ratio of fine root mass. Yet, it is likely that the bulk of partly decomposed FRN fragments in the samples originate from earlier die-off events, and that the <10 mm fraction is the one most influenced by the activity of decomposers in the soil. This suggested focusing on the larger, still intact necromass fragments (>10 mm length), which more likely were formed in summer 2018.

2.2.3. Fine Root Morphology

Four to five intact rootlets were picked from the living biomass fraction and further analysed for their mean root diameter, specific root surface area (SRA, in $cm^2\ g^{-1}$), specific root length (SRL, in $m\ g^{-1}$), root tissue density (in $g\ cm^{-3}$), and the number of root tips per mass using a water bath scanner and the WinRhizo (Régent Instruments Inc., Quebec, QC, Canada) visual analysis system. All morphological parameters were calculated on a dry biomass (70 °C for 48 h) basis.

2.3. Statistical Analyses

All calculations and tests were conducted with version 3.6.1 of R (R Core Team 2019). All fine root biomass, necromass, and morphological data showed a strong right-skewed distribution and were neither within the species, nor among plots and different species normally distributed. In some cases, the necromass values were almost bi-modally distributed, as root necromass distribution within the soil was highly patchy. We therefore used non-parametric tests to detect differences between years in fine root bio- and necromass. Since it is a priori unclear, whether two soil samples taken at short distance (40 cm) in two subsequent years are paired or independent, we decided to conduct two non-parametric tests: the Wilcoxon signed-rank test and the Wilcoxon-Mann-Whitney U test. Since both tests resulted in exactly the same pattern of significant differences, we here only report the results of the signed-rank test, because pair-wise comparison seems to better fit to the repeat-sampling strategy of this study.

In order to explore the relationships between various site-specific soil characteristics, tree size attributes, climate variables and fine root data, principal components analyses (PCA) were conducted separately for site- and species-level data for the 2017 and 2018 sampling campaigns (R-Packages "FactoExtra" and "FactoMineR", [63,64]). The PCA included the variables mean annual precipitation (MAP), mean annual temperature (MAT), de Martonne aridity index (DMI) of the 3 months prior to sampling, soil pH, C/N ratio, resin-exchangeable P concentration, organic matter content, silt content and soil bulk density (0–10 cm depth), mean tree height, diameter at breast height (DBH), FRB, FRN, N/B ratio, specific root area (SRA), and specific root length (SRL). To account for the right-skewed distribution of fine root data, we log-transformed, centred, and scaled all biomass, necromass, and morphological data prior to the PCA analysis.

Further, linear mixed effects models were fitted for the 2017 and 2018 data sets separately for all predictors and dependent variables (R-package lme4, [65]). The models included one of the predictors (MAP, MGSP, MAT, soil pH, soil C/N ratio, silt proportion, soil organic matter content, tree age, height, and DBH) and its interaction with the factor "species" as fixed effects, while the factor "site" was introduced as random effect. The random effect was introduced, because fine root data on tree level were nested within species per site. The dependent variables in the models were the log-scaled fine root mass and morphology data. Here, we only report the results of the models with MAP as predictor, as the other variables led either to very similar results (e.g., MGSP) or showed no significant effects and very small effect sizes. These minor inter-relationships among biotic, edaphic, and climatic variables in the data set are already demonstrated by the PCAs.

All models were checked for constant variance of the residuals across fitted values and between levels of the fixed effects, as well as for acceptable normality of the distribution of the residuals using Q-Q-plots. Only the model with fine root necromass as dependent variable showed slightly distorted residuals in part of the data set due to several very low necromass values, which did not apply to the model with necromass/biomass ratio. Conclusions from the N/B ratio model are thus more robust than

those from the necromass-only model. All estimates are based on the restricted maximum likelihood (REML) criterion and *p*-values were calculated with the lmerTest package based on Satterthwaites method [66].

Reported marginal "pseudo-R^2" values were calculated per species according to Nakagawa and Schielzeth [67] and represent a measure for explained variance of the fixed effects in mixed-effects models:

$$R^2_{marg} = 1 - \frac{variance\left(res_{marg}\right)}{variance(\log(variable))} \quad (1)$$

where res_{marg} are the residuals of the marginal predictions of the model.

3. Results

3.1. Fine Root Biomass, Necromass, and Morphology in the 2017 and 2018 Inventories

Across the nine sites, FRB density in the mineral topsoil (0–10 cm) was lowest in stands of *Q. petraea* and *T. cordata* (mostly in the range 0.2–0.8 g L^{-1}), intermediate in *A. platanoides* (0.3–2.0 g L^{-1}), and highest in *C. betulus* (0.8–2.0 g L^{-1}) and especially *F. excelsior* (1.5–4.0 g L^{-1}; Figure 2a). The corresponding FRB pools in the 0–10 cm layer were 20–80, 30–200, 80–200, and 150–400 g m^{-2}. Thus, across all sites, *F. excelsior* had about fivefold larger FRB densities in the topsoil than *Q. petraea*. The FRN pools (only fragments > 10 mm) were 10 to 100 times smaller than the biomass pools (Figure 2b), resulting in N/B ratios mostly in the range of 0.1 to 0.01 (Figure 2c).

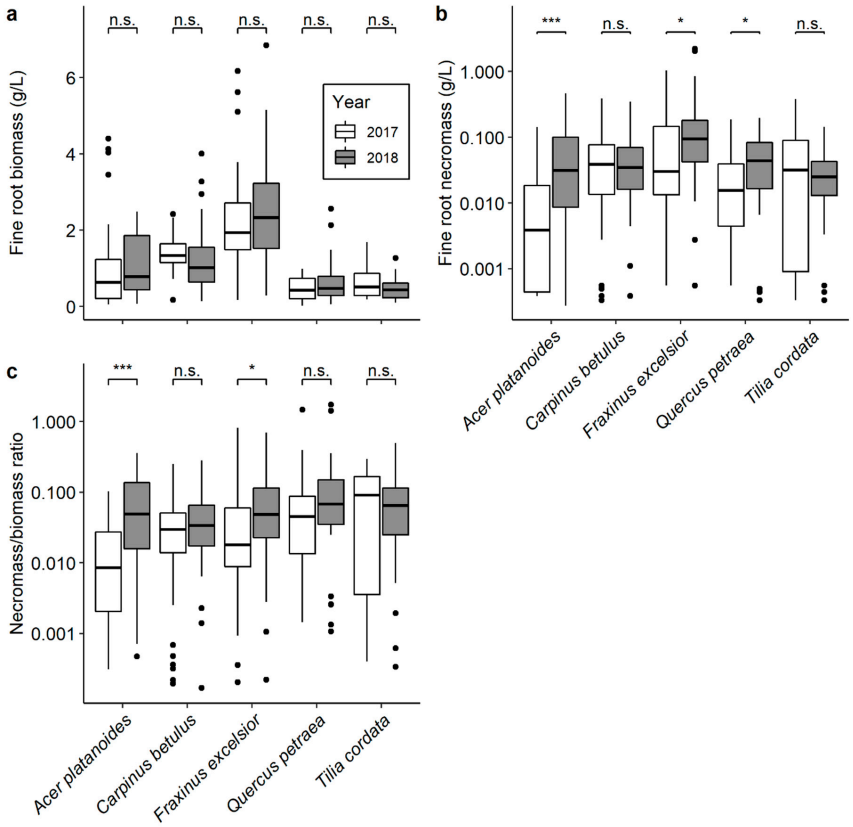

Figure 2. Fine root biomass (**a**), necromass (**b**), and necromass/biomass (N/B) ratio (**c**) of the five tree species in the topsoil (0–10 cm) in April 2017 and September 2018. Box-whisker plots with median and interquartile ranges (Q_1–Q_3); whiskers extend to 1.5 times the interquartile range. Indicated significant differences between the inventories for each species are based on a non-parametric signed-rank-test; ***: $p \leq 0.001$, *: $p < 0.05$. Note the log-scaled y-axes in (**b**) and (**c**).

Comparing the FRB recorded in the moist spring of 2017 to the biomass of the dry summer of 2018 revealed in none of the five species a significant difference, whereas necromass was significantly greater after the 2018 drought in three species (*A. platanoides*, *F. excelsior*, and *Q. petraea*) but unchanged in the other two (Figure 2a,b). The N/B ratio was higher after the 2018 drought in *A. platanoides* and *F. excelsior,* but not in the other three species (Figure 2c).

While FRN was not different between the two inventories in *C. betulus* and *T. cordata*, SRA was significantly smaller in these species after the 2018 drought than in 2017 (Figure 3a). A similar morphological response was observed also in *A. platanoides*, while the SRA of the other two species did not respond to the drought. All species except *Q. petraea* showed significantly reduced root tip numbers per FRB after the 2018 drought (Figure 3b).

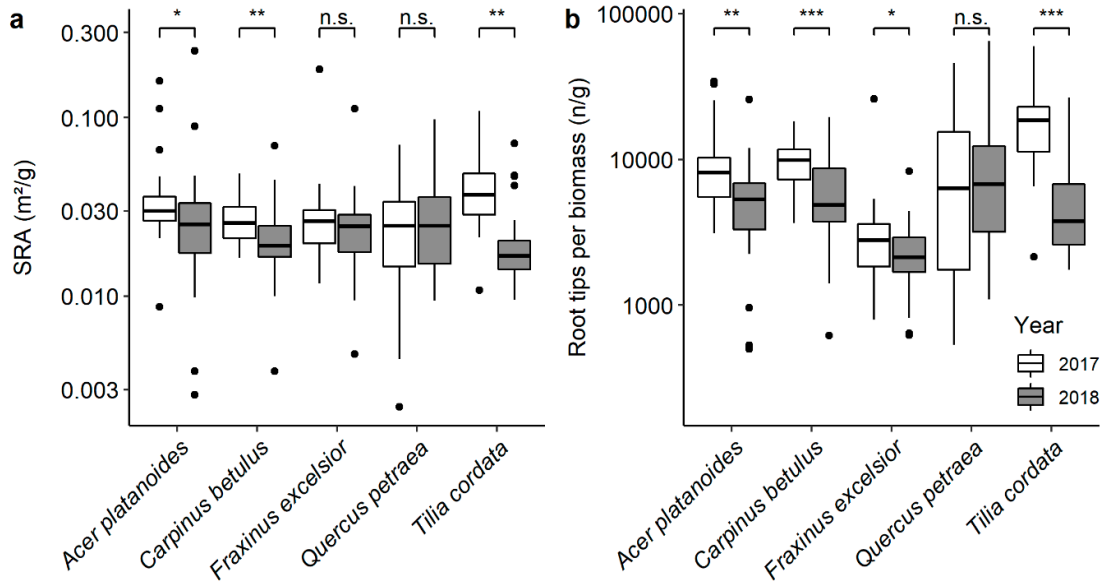

Figure 3. Specific root surface area (SRA) (**a**) and root tips per fine root biomass (**b**) of the five tree species in the topsoil (0–10 cm) in April 2017 and September 2018. Box-whisker plots for all species and both inventories with median and interquartile ranges (Q_1–Q_3); whiskers extend to 1.5 times the interquartile range. Indicated significant differences between the inventories for each species are based on a non-parametric signed-rank-test; ***: $p \leq 0.001$, **: $p \leq 0.01$, *: $p < 0.05$. Note the log-scaled y-axes.

3.2. Changes in Fine Root Mass and Root Traits along the Precipitation Gradient

Under conditions of ample soil moisture in the spring of 2017, FRB density at the nine sites revealed a positive relationship with MAP in case of *Q. petraea*, a negative relation in *A. platanoides*, and no significant relations in the other three species (Figure 4, Table 3). FRN density increased with a decrease in MAP in all species except *Q. petraea*, and so did the N/B ratio. After the summer drought in 2018, in contrast, we found no dependence of FRB, FRN and N/B ratio on MAP (Table 3) due to a marked increase in FRN at the moister end of the precipitation gradient (Figure 4). FRB changed relatively little between 2017 and 2018 in four species, but showed a marked increase at the moist end of the gradient in *A. platanoides* (Figure 4).

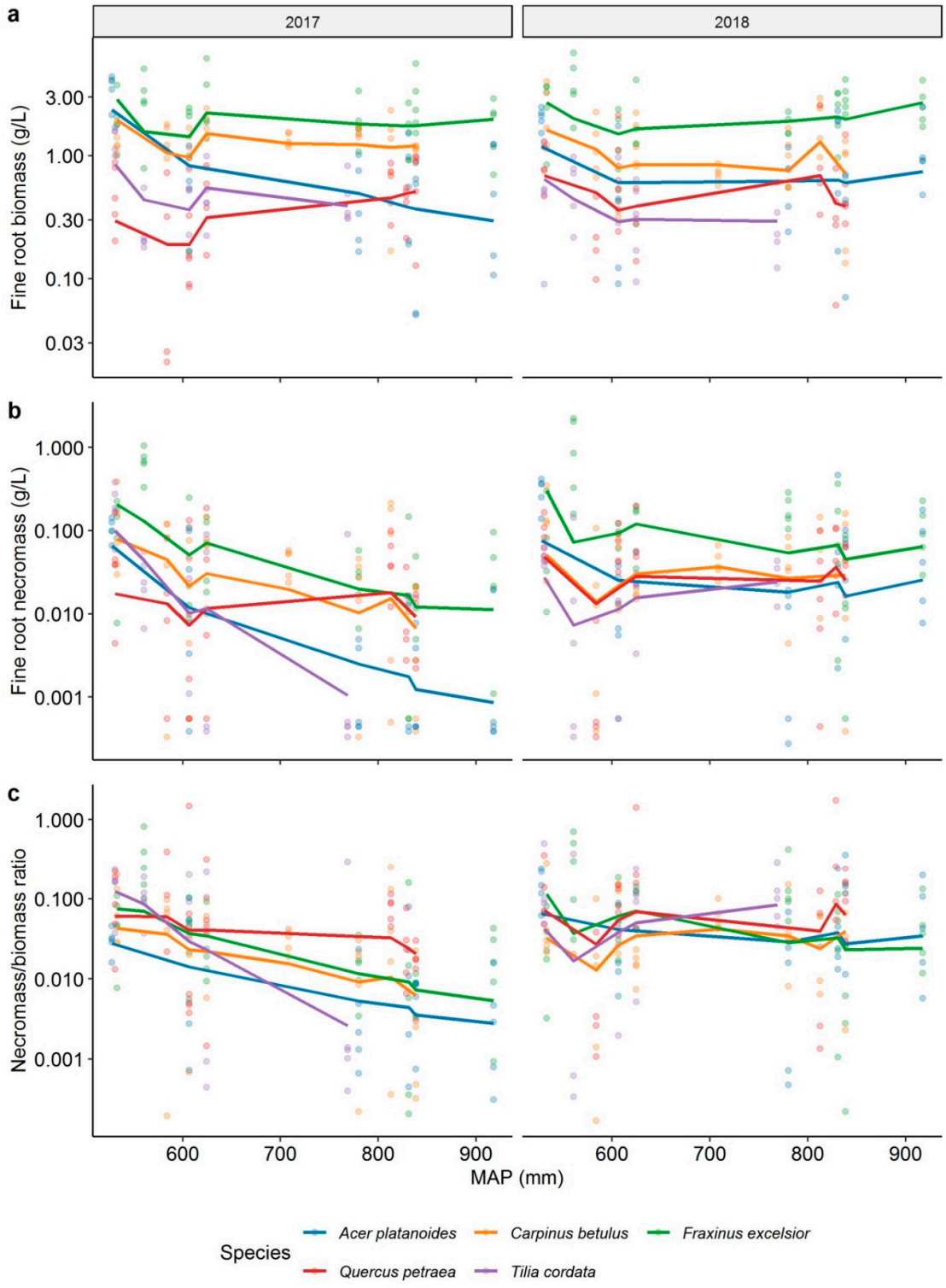

Figure 4. Fine root biomass (**a**), necromass (**b**), and necromass/biomass ratio (**c**) in the topsoil (0–10 cm) of the five species in relation to mean annual precipitation (MAP) in the 2017 and 2018 inventories. Data points are tree-level values, lines represent conditional predictions of the linear mixed effects model (the predictions of the fixed effect "MAP" for each species plus an intercept for each level of the random factor "site"). Note the log-scaled y-axis. The corresponding p and pseudo-R^2 values are summarized in Table 3. Graphs for the morphology variables are given in Figure A2 in the Appendix A.

Table 3. Results of linear mixed effects models for fine root traits in dependence of mean annual precipitation (MAP). Given are estimates of the fixed effect (fine root trait ~ species: MAP), marginal pseudo-R^2 for the fixed effect (calculated according to Nakagawa and Schielzeth (2013)), and *p*-values. *p*-values below 0.05 are given in bold. All fine root traits were log-transformed in advance except for root diameters.

Model ***Species***	**2017 (Moist)** **Estimate**	**Pseudo R^2**	***p*-Value**	**2018 (Dry)** **Estimate**	**Pseudo R^2**	***p*-Value**
Fine root biomass ~ MAP						
Fraxinus excelsior	−0.0004	0	0.678	0.0007	0	0.523
Carpinus betulus	−0.0004	0.02	0.752	−0.0009	0.03	0.531
Acer platanoides	−0.0048	0.31	**<0.001**	−0.0005	0.01	0.725
Quercus petraea	0.0029	0.12	**0.023**	−0.0001	0	0.933
Tilia cordata	−0.0024	0.07	0.264	−0.0021	0.1	0.368
Fine root necromass ~ MAP						
Fraxinus excelsior	−0.0074	0.32	**0.002**	−0.0034	0.07	0.147
Carpinus betulus	−0.0063	0.13	**0.032**	0.0011	0	0.711
Acer platanoides	−0.0113	0.47	**<0.001**	−0.0022	0.03	0.4
Quercus petraea	−0.0002	0	0.955	0.0005	0	0.841
Tilia cordata	−0.019	0.42	**<0.001**	0.0005	0	0.923
Necro-/biomass-ratio ~ MAP						
Fraxinus excelsior	−0.007	0.32	**<0.001**	−0.004	0.08	0.081
Carpinus betulus	−0.0057	0.11	**0.028**	0.002	0.01	0.482
Acer platanoides	−0.0063	0.25	**0.014**	−0.0016	0.02	0.523
Quercus petraea	−0.0029	0.05	0.211	0.0007	0	0.798
Tilia cordata	−0.0166	0.37	**<0.001**	0.0028	0.04	0.533
SRA ~ MAP						
Fraxinus excelsior	−0.001	0.09	0.15	−0.0006	0.03	0.367
Carpinus betulus	−0.0001	0	0.926	−0.0022	0.25	**0.011**
Acer platanoides	−0.0008	0.07	0.266	−0.0001	0	0.861
Quercus petraea	−0.002	0.1	**0.013**	−0.0013	0.09	0.117
Tilia cordata	0.0004	0	0.781	0.0001	0	0.918
Root tips per biomass ~ MAP						
Fraxinus excelsior	−0.0012	0.06	0.249	−0.0008	0.04	0.421
Carpinus betulus	−0.0006	0	0.648	−0.0038	0.35	**0.002**
Acer platanoides	−0.0015	0.11	0.179	−0.0006	0.01	0.587
Quercus petraea	−0.0043	0.16	**<0.001**	−0.0009	0.01	0.412
Tilia cordata	−0.0004	0.01	0.83	−0.0007	0.01	0.728
Root diameter ~ MAP						
Fraxinus excelsior	0.1511	0.02	0.269	0.2416	0.16	**0.014**
Carpinus betulus	0.1485	0.04	0.367	0.5943	0.51	**<0.001**
Acer platanoides	0.061	0	0.677	0.0426	0.01	0.7
Quercus petraea	0.5661	0.18	**<0.001**	0.0045	0	0.97
Tilia cordata	−0.0783	0	0.765	−0.0027	0	0.989

Of the root morphological traits, SRA and the number of root tips per biomass increased with decreasing MAP in the 2017 inventory in *Q. petraea,* and in 2018 in *C. betulus*, pointing at a larger absorptive capacity of the finest roots at drier sites (Table 3 and Figure A2 in the Appendix A). Accordingly, mean fine root diameter in the <2 mm category increased towards the moister sites. A similar pattern was also observed in the other species in both years, but the relationships were mostly not significant (exception: root diameter in *F. excelsior* in 2018) and the explained variance was low; especially *T. cordata* did not show significant morphological plasticity along the gradient (Table 3).

3.3. Interdependencies between Climatic and Edaphic Factors and Fine Root Variables along the Precipitation Gradient

The principal components analysis for the inventory in spring 2017 revealed a relatively continuous distribution of the study sites along the first three axes that explained 63.4% of the total variance of the dataset (Table 4, a graphical representation of the PCA results is provided in the Appendix A in Figure A3). The first axis (27.5% explained variance) coincided mainly with the climatic factors MAP and MAT and the weather prior to sampling (DMI). FRN and the N/B ratio were strongly correlated with the first axis as well, whereas root biomass itself and morphological attributes (SRA and SRL) coincided with the second axis (21.2% explained variance) and soil physical and chemical properties (C/N, silt content, bulk density, organic matter content). FRB was generally positively associated with

high organic matter content in the upper mineral soil and negatively influenced by high bulk density, which itself coincided with high silt content. The third axis (14.8% explained variance) reflects the positive association between tree height and soil pH and P availability, but did not correlate with climate or fine root variables.

Table 4. Results of the principal components analysis for the spring inventory in 2017. Given are the loadings of the selected variables along the four axes with the highest explained variance in the dataset. Bold numbers mark the variables with the highest loading (>0.4) on the respective axis. The values in brackets give the cumulative fraction of variance explained by the variable. MAP = mean annual precipitation, MAT = mean annual temperature, DMI = de Martonne aridity index of the three months prior to sampling.

Explained Variance:	**Axis 1 27.8%**		**Axis 2 21.1%**		**Axis 3 14.5%**		**Axis 4 12.8%**	
Climate factors								
MAP	**−0.93**	(0.86)	−0.03	(0.86)	−0.10	(0.88)	0.15	(0.9)
MAT	**0.86**	(0.74)	−0.07	(0.75)	0.36	(0.88)	0.06	(0.88)
DMI (sampling period)	**−0.92**	(0.84)	−0.10	(0.85)	−0.24	(0.9)	−0.02	(0.9)
Soil properties								
pH	−0.27	(0.07)	0.35	(0.2)	**0.70**	(0.69)	−0.06	(0.69)
C/N ratio	0.23	(0.05)	**−0.77**	(0.64)	−0.30	(0.73)	−0.11	(0.74)
Silt content (%)	0.01	(0)	**0.77**	(0.6)	−0.25	(0.66)	−0.03	(0.66)
P concentration	−0.24	(0.06)	0.11	(0.07)	**0.88**	(0.85)	0.19	(0.88)
Org. matter content	−0.25	(0.06)	**−0.70**	(0.55)	**0.47**	(0.77)	−0.12	(0.78)
Bulk density	0.33	(0.11)	**0.70**	(0.6)	−0.17	(0.63)	0.35	(0.75)
Stand structural parameters								
Tree height	−0.32	(0.1)	0.23	(0.15)	**0.48**	(0.39)	**0.55**	(0.69)
Diameter at breast height	0.20	(0.04)	**0.41**	(0.21)	−0.06	(0.21)	**0.59**	(0.56)
Fine root-related variables								
Fine root biomass	0.15	(0.02)	**−0.57**	(0.35)	0.29	(0.43)	0.06	(0.44)
Fine root necromass	**0.77**	(0.59)	−0.38	(0.73)	0.12	(0.75)	0.25	(0.81)
Fine root dead/live ratio	**0.86**	(0.74)	−0.06	(0.75)	−0.07	(0.75)	0.27	(0.82)
SRL	0.31	(0.1)	**0.45**	(0.3)	0.13	(0.31)	**−0.75**	(0.87)
SRA	0.25	(0.06)	0.39	(0.21)	0.33	(0.32)	**−0.69**	(0.8)

After the 2018 summer drought, the environmental and root-related variables in the data set were in general less tightly correlated to each other according to the PCA (Table 5, a graphical representation of the PCA results is provided in the Appendix A in Figure A4). The first axis (22.7% explained variance) coincided again mostly with climatic factors but did not explain root bio- or necromass variation. Instead, root morphological parameters had a reasonable loading on this axis (−0.67, −0.56). The second axis (21.1% explained variance) reflected influences of soil properties (C/N ratio, organic matter content, bulk density, soil texture) on FRB: The same positive effect of organic matter content and negative effect of bulk density as in 2017 was visible in this data set. Fine root bio- and necromass were strongly inter-related after the summer drought along the first two PCA axes in 2018, which relates to the relatively constant N/B ratio across plots and species in this inventory.

Stand and tree age was only weakly correlated with the studied fine root traits and we decided not to include it in the final PCAs to avoid mixing tree age/stand age data from different sources because dendrochronological determination of tree age was not possible for *C. betulus*.

Table 5. Results of the principal components analysis for the drought inventory in 2018. Given are the loadings of the selected variables along the four axes with the highest explained variance in the dataset. Bold numbers mark the variables with the highest loading (>0.4) on the respective axis. The values in brackets give the cumulative fraction of variance explained by the variable. MAP = mean annual precipitation, MAT = mean annual temperature, DMI = de Martonne aridity index of the three months prior to sampling.

Explained Variance:	**Axis 1 22.0%**		**Axis 2 21.6%**		**Axis 3 17.0%**		**Axis 4 11.4%**	
Climate factors								
MAP	**0.65**	(0.42)	0.25	(0.48)	−0.38	(0.62)	0.36	(0.75)
MAT	**−0.54**	(0.29)	−0.09	(0.3)	**0.65**	(0.72)	−0.26	(0.79)
DMI (sampling period)	**0.85**	(0.71)	−0.03	(0.72)	0.16	(0.74)	0.08	(0.75)
Soil properties								
pH	**0.69**	(0.48)	0.08	(0.48)	0.35	(0.61)	−0.37	(0.75)
C/N ratio	**−0.72**	(0.52)	**0.44**	(0.72)	−0.24	(0.78)	0.31	(0.87)
Silt content (%)	0.26	(0.07)	**−0.73**	(0.61)	−0.14	(0.63)	−0.12	(0.64)
P concentration	**0.59**	(0.35)	0.28	(0.43)	**0.59**	(0.78)	0.14	(0.81)
Org. matter content	−0.04	(0)	**0.84**	(0.71)	0.14	(0.73)	0.29	(0.82)
Bulk density	0.15	(0.02)	**−0.79**	(0.65)	0.12	(0.67)	−0.08	(0.67)
Stand structural parameters								
Tree height	**0.51**	(0.26)	0.02	(0.27)	**0.48**	(0.5)	**0.52**	(0.77)
Diameter at breast height	0.00	(0)	**−0.48**	(0.23)	0.39	(0.38)	0.36	(0.51)
Fine root-related variables								
Fine root biomass	−0.02	(0)	**0.56**	(0.32)	0.17	(0.35)	0.25	(0.41)
Fine root necromass	0.03	(0)	**0.65**	(0.42)	0.39	(0.57)	**−0.43**	(0.76)
Fine root dead/live ratio	0.05	(0)	0.33	(0.11)	0.33	(0.22)	**−0.70**	(0.71)
SRL	**−0.48**	(0.23)	−0.32	(0.33)	**0.59**	(0.68)	0.20	(0.72)
SRA	−0.38	(0.15)	−0.21	(0.19)	**0.72**	(0.7)	0.29	(0.79)

4. Discussion

4.1. Fine Root Biomass and Belowground C Allocation in Dependence on Long-Term Water Reduction

Our study at nine sites along the steep precipitation gradient in the rain shadow of the Harz mountains (MAP: 920–530 mm year^{-1}) found only weak support for optimal partitioning theory, when applied to the FRB stocks in the topsoil. FRB in the moist sampling period 2017 did not change in a consistent manner with decreasing mean annual precipitation. *A. platanoides* was the only species with a significant increase in FRB from the moister to the drier sites in 2017, which could point at increased belowground C allocation to increase water uptake, while *Q. petraea* showed a decrease and the other three species no relation of FRB to MAP. The outcome was not different when other precipitation variables (e.g., MGSP, current-year precipitation or climatic water balance) were used instead of the long-term mean. Other studies along precipitation gradients obtained mixed results, either no consistent change in FRB and relative C allocation to roots [68,69], a decrease [7,27], or an increase with decreasing water availability [26,33], suggesting a large influence of species and soil moisture conditions on the drought response of carbon allocation. Clearly, our fine root inventory covers only the topsoil and we hence may have missed preferential biomass partitioning to other parts of the root system. Trees growing at drier sites could allocate more carbon to root growth in deeper soil layers to access the moister subsoil and escape surface drying [70,71]. However, a meta-analysis of root biomass data by Schenk and Jackson [72] and a detailed study of the subsoil root system of *Fagus sylvatica* along a precipitation gradient by Meier et al. [68] showed the opposite response to long-term precipitation reduction, i.e., shallower rooting of trees under water limitation. An alternative explanation for the weak support for OPT in our study could be the only moderate length of the studied precipitation gradient (MAP difference: 390 mm year^{-1}), which apparently had only a minor effect on total tree productivity. Carbon allocations shifts in support of OPT were mostly found in studies across biomes or in experiments with very different treatments. Poorter et al. [73] concluded from a meta-analysis that marked increases in allocation to the root system occur only, when drought reduces biomass by 50 percent or more, which is not the case here.

The PCAs with root-related and environmental variables support the conclusion that the average soil moisture regime as indicated by the MAP gradient has only a minor influence on the FRB stocks at our study sites. In both root inventories, the association of FRB with edaphic and climatic variables suggests that topsoil FRB generally increases with organic matter content, but decreases with increasing nitrogen content, silt content and soil bulk density, while the effect of climatic factors (MAP, MAT) and also soil pH and P content is weak. This is in accordance with the observation that fine root density in temperate forest soils is usually highest in the carbon-rich Ah horizon and the organic layer with low bulk density [7,74].

Inherited tree species differences in FRB seem also to be more influential on FRB patterns than moisture conditions. In our study, *F. excelsior* had up to five times higher FRB densities in the topsoil than *Q. petraea* and *T. cordata*, with intermediate values in *C. betulus* and *A. platanoides*. While part of this variation may be due to differences in DBH and small-scale variations in stem density between species in mixed stands, comparison with earlier fine root studies in mixed forests suggests that the high FRB of *F. excelsior* and the low values of *Q. petraea* may be species-specific. This is indicated by a meta-analysis of fine root studies from temperate forests [8] and root inventories in mixed forests [54,75]. An additional explanation for low FRB values of *Q. petraea* might be a different depth distribution of fine roots, as other authors state that Central European oak species are generally deeper rooted than beech and other broadleaf tree species [76], but precise data on depth-distributions are lacking for our sites. The contrasting FRB patterns of *A. platanoides* and *Q. petraea* along the precipitation gradient further indicate that co-occurring tree species may differ not only in standing FRB but also in root mortality and the response of their carbon allocation modes to long-term reduction in water availability.

As predicted (hypothesis 1), all five species showed increasing amounts of FRN and an increasing N/B ratio in the topsoil with a decrease in MAP, while FRB remained unchanged (with the exception of *A. platanoides*). One possible explanation of this pattern is that fine root mortality increases with a permanent reduction in water availability, as has been observed in many field studies (e.g., [27]) and concluded from literature reviews (e.g., [36,77]), which in turn may trigger increased carbon allocation to root growth in compensation of the FRB loss. This was observed, for example, in Norway spruce roots under mild drought stress (soil matrix potentials of—0.06 MPa, [45]). Such a response will reduce mean fine root age and likely increase the water and nutrient uptake capacity of the tree and thus its fitness under water shortage [6,39]. Another possible explanation is fine root shedding with the assumed function to uncouple the rest of the hydraulic system from very low water potentials in dry soil to avoid embolism formation in more valuable organs (hydraulic fuse theory, [41,42]). It could take place during more severe drought events and does not imply the immediate replacement by new fine roots. In support of this idea, McCormack and Guo [36] predicted on the basis of a conceptual model exponential increases in root mortality at the highest drought stress intensities. This is in accordance with the results of a rainfall exclusion experiment with *Picea abies* trees, in which, under mild drought, root mortality increased, while fine root production was also stimulated. Under more severe drought, root mortality was high and no replacement occurred [45].

Our data suggest that the five species differ in specific root mortality rates upon soil desiccation, as the N/B ratio showed a more than tenfold increase with the MAP reduction along the transect in *T. cordata*, intermediate N/B slopes in *C. betulus*, *A. platanoides*, and *F. excelsior*, and the lowest increase in *Q. petraea*. We interpret these patterns as a hint that *Q. petraea* is better able than the other species to produce fine roots capable of tolerating long-term reductions in soil moisture without suffering increased root mortality. Physiological and genetic studies have to show whether this is due to a principally different physiological constitution of the fine roots of this ring-porous species, or is caused by the specific acclimation or adaptation of different oak populations along the precipitation gradient. An alternative explanation for increasing FRN amounts and N/B ratios with a MAP reduction is that the drier and somewhat warmer climate toward the east of the transect reduces root decomposition rate and thus leads to the accumulation of FRN, independent of changes in root mortality rate. In the absence of decomposition data, this possibility cannot be ruled out, but it is not very likely. The

gradients in MAT (7.9–9.9 °C), soil pH (4.2–6.5) and C/N ratio (10.7–18.9) along the transect were only moderate and the latter factors did not covary significantly, either with MAP or FRN. Moreover, site differences in decomposition rate should mainly affect the finest root necromass particles, which were not investigated here. We assume that the analyzed larger, less fragmented necromass fractions (>10 mm length) reflect more directly the root mortality processes, where decomposition likely has started only very recently.

4.2. Effects of the 2018 Summer Drought on Fine Root Biomass and Belowground C Allocation

It is noteworthy that none of the species showed a decrease in mean FRB across the transect after the severe 2018 summer drought (in *C. betulus*, a non-significant tendency for a decrease existed). The 2018 drought with summer precipitation amounts 55–73 % lower than the long-term average was extreme and resulted in the local dieback of more sensitive tree species (*Picea abies*, *Fagus sylvatica*) in the region. This indicates that all five species must be relatively tolerant of soil desiccation compared to other major timber species, and that precipitation is playing only a secondary role for the standing FRB of these species. It is possible that our FRB figures are influenced by temperature and other seasonal influences unrelated to summer drought, as fine root production and biomass stocks typically peak between April and July in central European broadleaf tree species, as is visible from studies in beech [27,78] and beech-oak mixed forests [38]. Thus, we cannot exclude with certainty that the biomass figures observed in September 2018 represent reduced values which are influenced by the typical seasonal FRB decrease that should have taken place later in summer. However, we did not observe a FRB reduction. Moreover, if the reduction had occurred, it should have been similar along the transect. In addition, the *A. platanoides* data from the moist transect end indicate the opposite, a FRB increase from the 2017 to the 2018 inventory.

Higher FRN amounts in three of the species (*A. platanoides*, *F. excelsior*, and *Q. petraea*) in 2018 (in comparison to 2017) indicate that drought has increased root mortality. Interestingly, the severe drought drove all N/B ratios to converge on a higher level, or, in other words, all species lost the MAP dependence of necromass and N/B ratio after the drought. This suggests that the mortality increase was greater at the moister than the drier sites in all species except for *Q. petraea*, which largely supports hypothesis 3. We explain this pattern with a generally higher drought sensitivity of the root systems at MAP > ca. 700 mm year^{-1}, which caused higher root mortality and leveled all FRN differences that exist along the transect in normal years. In *T. cordata* and *C. betulus*, FRN and N/B ratio were also higher at the moister sites in 2018 than 2017, but this response was compensated by lower FRN amounts at the drier sites. Thus, our second hypothesis is only partly supported.

In a meta-analysis about stand- and soil-related drivers of fine root N/B ratio across biomes, Wang et al. [37] found elevated N/B ratios at reduced precipitation only in forests dominated by ECM tree species, but not in AM forests. This suggests an influence of mycorrhizal type on the drought response of the root system. Liese et al. [79] confirmed these findings in a mesocosm experiment for several temperate tree species (including *Acer*, *Fraxinus*, *Carpinus*, *Tilia*, and *Quercus* taxa), demonstrating a much greater drought-induced root lifespan reduction in ECM than AM species (40–56% vs. 0.5–13%). Our data from three ECM (*C. betulus*, *T. cordata*, and *Q. petraea*) and two AM species (*A. platanoides* and *F. excelsior*) do not support this conclusion, as *Q. petraea* was the species with the smallest N/B response to a MAP reduction at the drier end of the gradient. The response to the 2018 summer drought even revealed the opposite response pattern to that found by Wang et al. [37] and Liese et al. [79], with a significant increase in the N/B ratios in the AM species *A. platanoides* and *F. excelsior*, while all ECM species did not respond. One possible explanation for the discrepancy between the results of the Wang et. [37] and Liese et al. [79] studies and our investigation is that largely different spatial scales (comparison of biomes with different climates; sapling experiment; regional gradient study) are considered.

4.3. Root Morphological Change in Response to Reduced Water Availability

Trees can adapt to shortages in water or nutrients by increasing the absorptive capacity of the root system in two different ways: by enhancing root production and maintaining larger absorbing surface areas (extensive strategy), or by modifying root morphology and physiology in order to increase uptake efficiency per root mass (intensive strategy, [80,81]). In contrast to the other four species, *Q. petraea* showed characteristics of an intensive adaptation strategy by increasing SRA and the number of root tips per root mass towards the drier sites according to the 2017 inventory, while FRB remained constant. *Q. petraea* differed further from the other species by showing no root tip shedding and no SRA reduction after the 2018 drought. *A. platanoides* showed the opposite response with a FRB increase towards the drier sites, while root morphology was not altered. The other three species maintained a constant FRB along the gradient, but the marked FRN increase toward the drier sites points at elevated root turnover and compensatory stimulation of fine root production under desiccation, which can be viewed as attributes of an extensive strategy.

After the 2018 drought, all species except *Q. petraea* showed a marked dieback of root tips and more distal thin rootlets. This resulted in the observed SRA reduction, which was particularly strong in *T. cordata*. The losses in the putatively most active finest rootlets had not been replaced until September 2018, when sampling was conducted. We interpret this response in 2018 as an indicator of belowground vulnerability to extreme drought, which must have reduced the vitality and absorptive capacity of the fine root system of *F. excelsior*, *A. platanoides*, *C. betulus*, and *T. cordata*.

4.4. Species Differences in the Belowground Drought Response

The fine root system of *Q. petraea* seems to be more resistant to both permanent moisture reduction and severe drought events than that of *T. cordata*, *C. betulus*, *F. excelsior*, and *A. platanoides* due to the following features: (1) Although fine root necromass increased after the 2018 summer drought, the N/B ratio changed only a little and it was roughly constant across the precipitation gradient. (2) Fine root morphology and the number of root tips were not affected by the drought, indicating either low sensitivity or rapid recovery in oak roots. This fits to findings from the dendrochronological analysis of climate sensitivity (e.g., [82]) and more general comparative assessments of drought resistance of the species based on climate envelopes [1,83]. On the other hand, *Q. petraea* maintained the lowest fine root density in the topsoil and more generally seems to produce a relatively small fine root system. Due to still-unknown morphological and/or physiological properties, oak can also maintain its fine roots in dry periods instead of shedding and partly replacing them. This rather "conservative" strategy with lower maintenance costs and a more or less constant root biomass during wet and dry periods was also observed in other Central European oak forests by Leuschner et al. [75], who compared *Q. petraea* to *Fagus sylvatica* and concluded that this strategy comes with the drawback of inferior interspecific competitive ability.

The other four species have in common that they all show indications of a somewhat greater belowground vulnerability to severe soil drought, but they pursue different strategies. *T. cordata* seems to be the most vulnerable species due to large drought-induced reductions in SRA and tip frequency, which is in line with assessments based on leaf and stem level data [84,85]. *F. excelsior* is unique due to its high fine root density, which may secure water uptake in drought periods and increase the species' competitive ability in mixed stands and on very shallow and dry soils.

5. Conclusions

Our results suggest that co-occurring tree species differ in the drought sensitivity of their fine root systems, which could play an important role with respect to the species' fitness and drought survival. Yet, much less is known about the belowground growth and stress tolerance strategies of trees than about aboveground responses.

This case study suffers from a number of shortcomings that are introduced with the study design and the methods used, which may bias some of the conclusions. First, the study design is not fully symmetric, as not all tree species occur at all sites, which weakens the power of statistical analysis. Second, our FRN analysis covers only the larger fragments, as the finest particles could not be identified to the species level. Consideration of the complete root necromass pool might have led to somewhat different results. Finally, edaphic inhomogeneity introduces some noise in the climatic signal retrieved from the precipitation gradient, which may weaken some of the conclusions. Fortunately, climate and soil properties did not covary systematically. While the retrieved patterns seem plausible, they need verification by additional gradient studies in other regions and with additional species.

We conclude that the comparative analysis of fine root biomass, necromass, and fine root morphology along precipitation gradients, and in moist and dry periods, has the potential to provide valuable information on the belowground drought sensitivity of tree species, thereby complementing results from canopy- and leaf-level studies.

Author Contributions: Conceptualization, C.L., S.F., D.H., B.S.; Data curation, S.F.; Formal analysis, S.F.; Funding acquisition, C.L.; Investigation, S.F.; Methodology, S.F. and D.H.; Project administration, B.S. and C.L.; Supervision, D.H., B.S., and C.L.; Validation, S.F. and C.L.; Visualization, S.F.; Writing—original draft, S.F. and C.L.; Writing—review and editing, S.F., C.L., and D.H. All authors have read and agreed to the published version of the manuscript.

Funding: This research was funded by the Bundesministerium für Ernährung und Landwirtschaft (Germany), Bundesministerium für Umwelt, Naturschutz und nukleare Sicherheit (Germany) and the Fachagentur Nachwachsende Rohstoffe e. V. (Germany) within the frame of the "Waldklimafonds".

Acknowledgments: Many thanks go to Irmgard Gerstmann and Mechthild Stange for their skillful support with the fine root analysis. We gratefully acknowledge the financial support granted by the Bundesministerium für Ernährung und Landwirtschaft (Germany), Bundesministerium für Umwelt, Naturschutz und nukleare Sicherheit (Germany) and the Fachagentur Nachwachsende Rohstoffe e. V. (Germany) within the frame of the "Waldklimafonds" (project DIVforCLIM). Additionally, we thank the local forestry authorities of Lower Saxony and Saxony-Anhalt and the DBU-Naturerbe GmbH for permissions to conduct the study, and the Nordwestdeutsche Forstliche Versuchsanstalt for kindly providing forest inventory data for the identification of suitable study sites.

Conflicts of Interest: The authors declare no conflict of interest. The funders had no role in the design of the study; in the collection, analyses, or interpretation of data; in the writing of the manuscript, or in the decision to publish the results.

Appendix A

Table A1. Results of linear mixed effects models for fine root bio- and necromass in dependence of actual precipitation in the year prior to sampling (act.PRCP). Given are estimates of the fixed effect (fine root trait ~ species:MAP), marginal pseudo-R^2 for the fixed effect (calculated according to Nakagawa and Schielzeth (2013)), and p-values. p-values below 0.05 are given in bold. All fine root traits were log-transformed in advance.

Model	2017 (Moist)			2018 (Dry)		
Species	Estimate	Pseudo r^2	p-Value	Estimate	Pseudo r^2	p-Value
Fine root biomass ~ act.PRCP						
Fraxinus excelsior	−0.0003	0.00	0.805	0.0007	0.00	0.543
Carpinus betulus	−0.0007	0.03	0.650	−0.0008	0.02	0.544
Acer platanoides	−0.0066	0.33	**<0.001**	−0.0006	0.02	0.630
Quercus petraea	0.0041	0.15	**0.013**	0.0003	0.00	0.824
Tilia cordata	−0.0028	0.04	0.313	−0.0015	0.07	0.447
Fine root necromass ~ act.PRCP						
Fraxinus excelsior	−0.0096	0.30	**0.003**	−0.0032	0.06	0.152
Carpinus betulus	−0.0087	0.14	**0.017**	0.0013	0.00	0.622
Acer platanoides	−0.0147	0.48	**<0.001**	−0.0031	0.06	0.227
Quercus petraea	−0.0001	0.00	0.975	0.0008	0.00	0.750
Tilia cordata	−0.0247	0.43	**<0.001**	0.0000	0.00	0.994
Necro-/biomass-ratio ~ act.PRCP						
Fraxinus excelsior	−0.0094	0.32	**<0.001**	−0.0038	0.07	0.089
Carpinus betulus	−0.0077	0.12	**0.014**	0.0021	0.01	0.415
Acer platanoides	−0.0079	0.24	**0.009**	−0.0024	0.04	0.345
Quercus petraea	−0.0040	0.06	0.192	0.0005	0.00	0.825
Tilia cordata	−0.0220	0.40	**<0.001**	0.0017	0.03	0.668

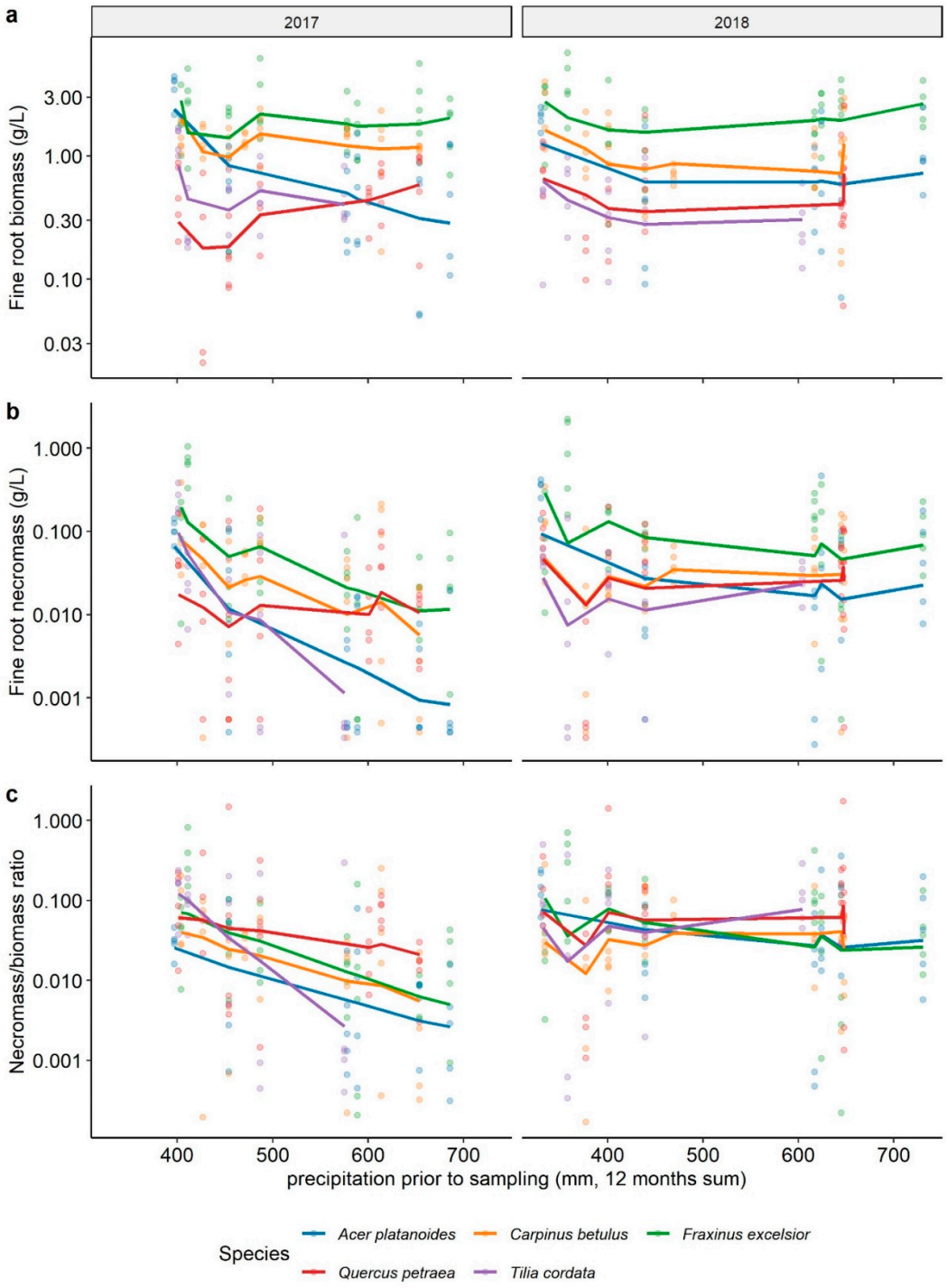

Figure A1. Fine root biomass (**a**), necromass (**b**) and necromass/biomass ratio (**c**) in the topsoil (0–10 cm) of the five species in relation to actual precipitation in the year prior to sampling in the 2017 and 2018 inventories. Data points are tree-level values, lines represent conditional predictions of the linear mixed effects model (the predictions of the fixed effect "MAP" for each species plus an intercept for each level of the random factor "site"). Note the log-scaled y-axis. The corresponding p and pseudo-R^2 values are summarized in Table A1.

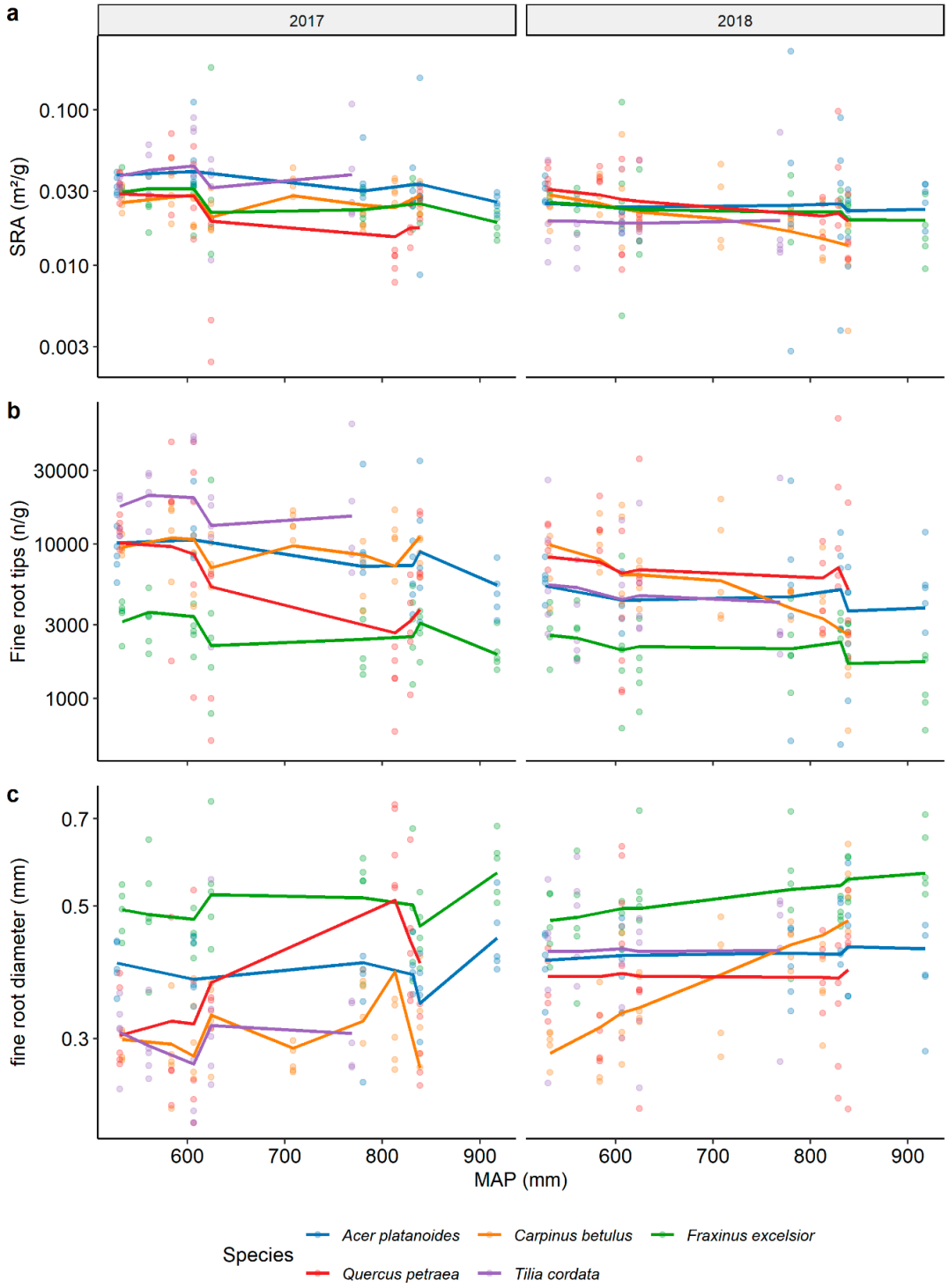

Figure A2. Specific root area (**a**), fine root tips per root mass (**b**), and average fine root diameter (**c**) in the topsoil (0–10 cm) of the five species in relation to mean annual precipitation (MAP) in the 2017 and 2018 inventories. Data points are tree-level values, lines represent conditional predictions of the linear mixed effects model (the predictions of the fixed effect "MAP" for each species plus an intercept for each level of the random factor "site"). Note the log-scaled y-axis. The corresponding p and pseudo-R^2 values are summarized in Table 3.

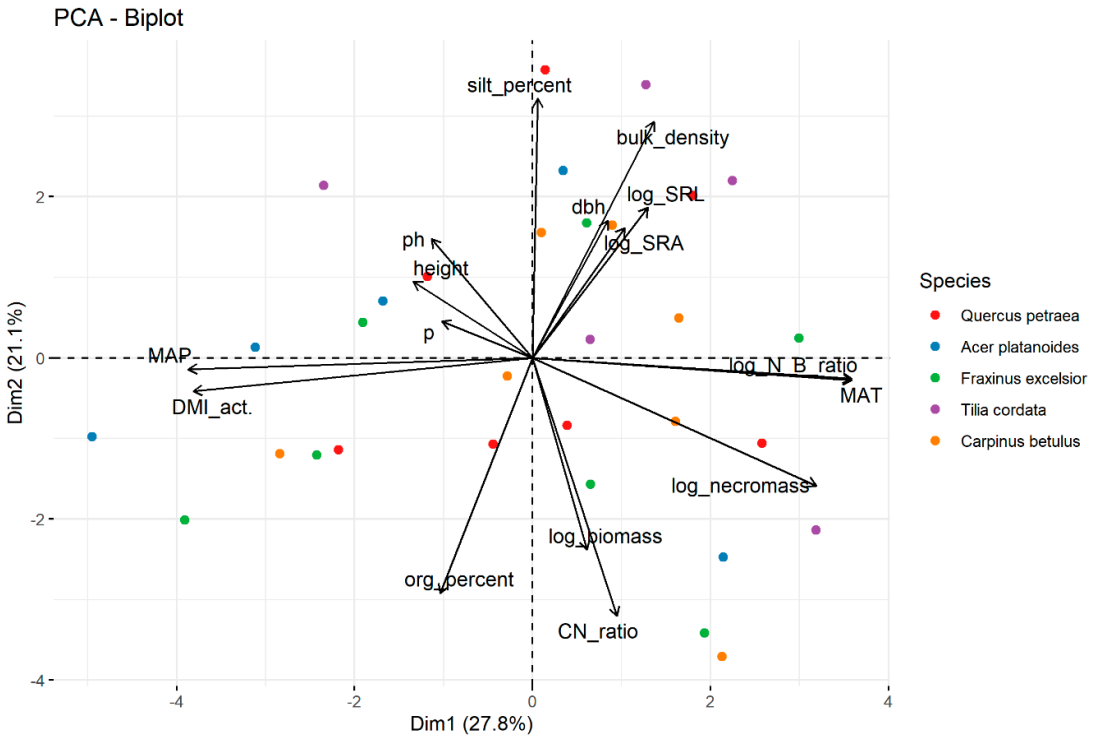

Figure A3. Principal components analysis (PCA) biplot of the 2017 fine root inventory. All data are aggregated on site and species level.

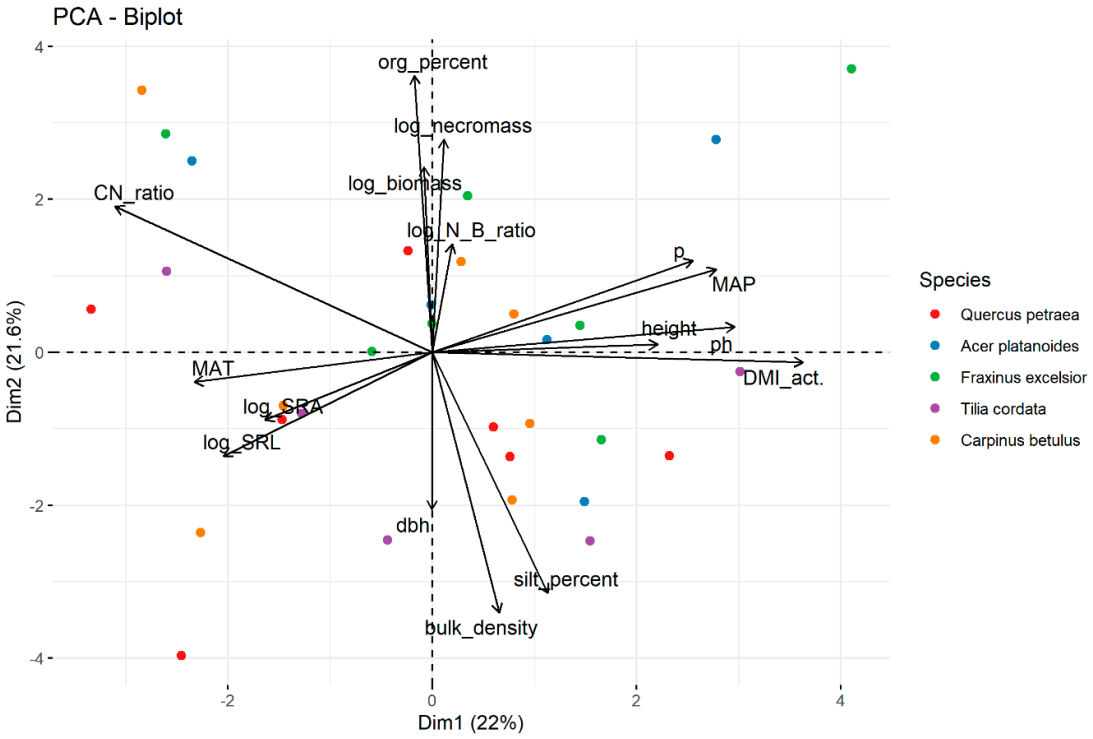

Figure A4. PCA biplot of the 2018 fine root inventory. All data are aggregated on site and species level.

References

1. Leuschner, C.; Ellenberg, H. *Ecology of Central European Forests: Vegetation Ecology of Central Europe*; Springer International Publishing: Cham, Switzerland, 2017; Volume I.

2. Jackson, R.B.; Mooney, H.A.; Schulze, E.D. A global budget for fine root biomass, surface area, and nutrient contents. *Proc. Natl. Acad. Sci. USA* **1997**, *94*, 7362–7366. [CrossRef]
3. Nadelhoffer, K.J.; Raich, J.W. Fine Root Production Estimates and Belowground Carbon Allocation in Forest Ecosystems. *Ecology* **1992**, *73*, 1139–1147. [CrossRef]
4. Rasse, D.P.; Rumpel, C.; Dignac, M.-F. Is soil carbon mostly root carbon? Mechanisms for a specific stabilisation. *Plant Soil* **2005**, *269*, 341–356. [CrossRef]
5. Eissenstat, D.M.; Yanai, R.D. Root life span, efficiency, and turnover. In *Plant Roots: The Hidden Half*, 3rd ed.; Kafkafi, U., Waisel, Y., Eshel, A., Eds.; CRC Press: Boca Raton, FL, USA, 2002; pp. 221–238, ISBN 978-0-8247-0631-9.
6. Brunner, I.; Herzog, C.; Dawes, M.A.; Arend, M.; Sperisen, C. How tree roots respond to drought. *Front. Plant Sci.* **2015**, *6*, 547. [CrossRef] [PubMed]
7. Leuschner, C.; Hertel, D.; Schmid, I.; Koch, O.; Muhs, A.; Hölscher, D. Stand fine root biomass and fine root morphology in old-growth beech forests as a function of precipitation and soil fertility. *Plant Soil* **2004**, *258*, 43–56. [CrossRef]
8. Leuschner, C.; Hertel, D. Fine Root Biomass of Temperate Forests in Relation to Soil Acidity and Fertility, Climate, Age and Species. *Prog. Bot.* **2003**, *64*, 405–438. [CrossRef]
9. Pregitzer, K.S.; Hendrick, R.L.; Fogel, R. The demography of fine roots in response to patches of water and nitrogen. *New Phytol.* **1993**, *125*, 575–580. [CrossRef]
10. IPCC. Contribution of working group II to the fifth assessment report of the intergovernmental panel on climate change. In *Climate Change 2014: Impacts, Adaptation and Vulnerability*; Field, C.B., Barros, V.R., Dokken, D.J., Mach, K.J., Mastrandrea, M.D., Bilir, T.E., Monalisa, C., Kristie, L.E., Yuka, O.E., Robert, C.G., et al., Eds.; Cambridge University Press: New York, NY, USA, 2014; ISBN 978-1-107-64165-5.
11. Schär, C.; Vidale, P.L.; Lüthi, D.; Frei, C.; Häberli, C.; Liniger, M.A.; Appenzeller, C. The role of increasing temperature variability in European summer heatwaves. *Nature* **2004**, *427*, 332–336. [CrossRef]
12. Ryan, M.G. Tree responses to drought. *Tree Physiol.* **2011**, *31*, 237–239. [CrossRef]
13. Senf, C.; Pflugmacher, D.; Zhiqiang, Y.; Sebald, J.; Knorn, J.; Neumann, M.; Hostert, P.; Seidl, R. Canopy mortality has doubled in Europe's temperate forests over the last three decades. *Nat. Commun.* **2018**, *9*, 4978. [CrossRef]
14. Anderegg, W.R.L.; Kane, J.M.; Anderegg, L.D.L. Consequences of widespread tree mortality triggered by drought and temperature stress. *Nat. Clim. Chang.* **2013**, *3*, 30–36. [CrossRef]
15. Allen, C.D.; Macalady, A.K.; Chenchouni, H.; Bachelet, D.; McDowell, N.; Vennetier, M.; Kitzberger, T.; Rigling, A.; Breshears, D.D.; Hogg, E.H.; et al. A global overview of drought and heat-induced tree mortality reveals emerging climate change risks for forests. *For. Ecol. Manag.* **2010**, *259*, 660–684. [CrossRef]
16. Reich, P. Root–Shoot Relations. In *Plant Roots: The Hidden Half*, 3rd ed.; Kafkafi, U., Waisel, Y., Eshel, A., Eds.; CRC Press: Boca Raton, FL, USA, 2002; pp. 205–220, ISBN 978-0-8247-0631-9.
17. Bloom, A.J.; Chapin, F.S.; Mooney, H.A. Resource Limitation in Plants-An Economic Analogy. *Annu. Rev. Ecol. Syst.* **1985**, *16*, 363–392. [CrossRef]
18. Mokany, K.; Raison, R.J.; Prokushkin, A.S. Critical analysis of root: Shoot ratios in terrestrial biomes. *Glob. Chang. Biol.* **2006**, *12*, 84–96. [CrossRef]
19. Kozlowski, T.T.; Pallardy, S.G. Acclimation and Adaptive Responses of Woody Plants to Environmental Stresses. *Bot. Rev.* **2002**, *68*, 270–334. [CrossRef]
20. Hertel, D.; Therburg, A.; Villalba, R. Above- and below-ground response by Nothofagus pumilio to climatic conditions at the transition from the steppe–forest boundary to the alpine treeline in southern Patagonia, Argentina. *Plant Ecol. Divers.* **2008**, *1*, 21–33. [CrossRef]
21. Coomes, D.A.; Grubb, P.J. Impacts of root competition in forests and woodlands: A theoretical framework and review of experiments. *Ecol. Monogr.* **2000**, *70*, 171–207. [CrossRef]
22. Thomas, F.M.; Gausling, T. Morphological and physiological responses of oak seedlings (*Quercus petraea* and *Q. robur*) to moderate drought. *Ann. For. Sci.* **2000**, *57*, 325–333. [CrossRef]
23. Tomlinson, P.T.; Anderson, P.D. Ontogeny affects response of northern red oak seedlings to elevated CO2 and water stress: II. Recent photosynthate distribution and growth. *New Phytol.* **1998**, *140*, 493–504. [CrossRef]
24. van Hees, A.F.M. Growth and morphology of pedunculate oak (*Quercus robur* L) and beech (*Fagus sylvatica* L) seedlings in relation to shading and drought. *Ann. For. Sci.* **1997**, *54*, 9–18. [CrossRef]

25. Kuster, T.M.; Arend, M.; Günthardt-Goerg, M.S.; Schulin, R. Root growth of different oak provenances in two soils under drought stress and air warming conditions. *Plant Soil* **2013**, *369*, 61–71. [CrossRef]
26. Hertel, D.; Strecker, T.; Müller-Haubold, H.; Leuschner, C. Fine root biomass and dynamics in beech forests across a precipitation gradient—is optimal resource partitioning theory applicable to water-limited mature trees? *J. Ecol.* **2013**, *101*, 1183–1200. [CrossRef]
27. Meier, I.C.; Leuschner, C. Belowground drought response of European beech: Fine root biomass and carbon partitioning in 14 mature stands across a precipitation gradient. *Glob. Chang. Biol.* **2008**, *14*, 2081–2095. [CrossRef]
28. Zang, U.; Goisser, M.; Häberle, K.-H.; Matyssek, R.; Matzner, E.; Borken, W. Effects of drought stress on photosynthesis, rhizosphere respiration, and fine-root characteristics of beech saplings: A rhizotron field study. *J. Plant Nutr. Soil Sci.* **2014**, *177*, 168–177. [CrossRef]
29. Meier, I.C.; Leuschner, C. Genotypic variation and phenotypic plasticity in the drought response of fine roots of European beech. *Tree Physiol.* **2008**, *28*, 297–309. [CrossRef] [PubMed]
30. Aspelmeier, S.; Leuschner, C. Genotypic variation in drought response of silver birch (*Betula pendula Roth*): Leaf and root morphology and carbon partitioning. *Trees* **2006**, *20*, 42–52. [CrossRef]
31. Bongarten, B.C.; Teskey, R.O. Dry weight partitioning and its relationship to productivity in loblolly pine seedlings from seven sources. *For. Sci.* **1987**, *33*, 255–267.
32. Bakker, M.R.; Augusto, L.; Achat, D.L. Fine root distribution of trees and understory in mature stands of maritime pine (*Pinus pinaster*) on dry and humid sites. *Plant Soil* **2006**, *286*, 37–51. [CrossRef]
33. Parker, M.M.; van Lear, D.H. Soil Heterogeneity and Root Distribution of Mature Loblolly Pine Stands in Piedmont Soils. *Soil Sci. Soc. Am. J.* **1996**, *60*, 1920. [CrossRef]
34. Chenlemuge, T.; Hertel, D.; Dulamsuren, C.; Khishigjargal, M.; Leuschner, C.; Hauck, M. Extremely low fine root biomass in Larix sibirica forests at the southern drought limit of the boreal forest. *Flora Morphol. Distrib. Funct. Ecol. Plants* **2013**, *208*, 488–496. [CrossRef]
35. Santantonio, D.; Hermann, R.K. Standing crop, production, and turnover of fine roots on dry, moderate, and wet sites of mature Douglas-fir in western Oregon. *Ann. For. Sci.* **1985**, *42*, 113–142. [CrossRef]
36. McCormack, M.L.; Guo, D. Impacts of environmental factors on fine root lifespan. *Front. Plant Sci.* **2014**, *5*, 205. [CrossRef] [PubMed]
37. Wang, C.; Chen, Z.; Yin, H.; Guo, W.; Cao, Y.; Wang, G.; Sun, B.; Yan, X.; Li, J.; Zhao, T.-H.; et al. The Responses of Forest Fine Root Biomass/Necromass Ratio to Environmental Factors Depend on Mycorrhizal Type and Latitudinal Region. *J. Geophys. Res. Biogeosci.* **2018**, *123*, 1769–1788. [CrossRef]
38. Hertel, D.; Leuschner, C. A comparison of four different fine root production estimates with ecosystem carbon balance data in a Fagus-Quercus mixed forest. *Plant Soil* **2002**, *239*, 237–251. [CrossRef]
39. Eissenstat, D.M.; Wells, C.E.; Yanai, R.D.; Whitbeck, J.L. Building roots in a changing environment: Implications for root longevity. *New Phytol.* **2000**, *147*, 33–42. [CrossRef]
40. Rewald, B. Impact of Climate Change-Induced Drought on Tree Root Hydraulic Properties and Competition Belowground. Ph.D. Thesis, Georg-August-University, Goettingen, Germany, 2008.
41. Jackson, R.B.; Sperry, J.S.; Dawson, T.E. Root water uptake and transport: Using physiological processes in global predictions. *Trends Plant Sci.* **2000**, *5*, 482–488. [CrossRef]
42. Alder, N.N.; Sperry, J.S.; Pockman, W.T. Root and stem xylem embolism, stomatal conductance, and leaf turgor in Acer grandidentatum populations along a soil moisture gradient. *Oecologia* **1996**, *105*, 293–301. [CrossRef]
43. Persson, H.Å.; Stadenberg, I. Fine root dynamics in a Norway spruce forest (*Picea abies* (L.) Karst) in eastern Sweden. *Plant Soil* **2010**, *330*, 329–344. [CrossRef]
44. Puhe, J. Growth and development of the root system of Norway spruce (*Picea abies*) in forest stands—A review. *For. Ecol. Manag.* **2003**, *175*, 253–273. [CrossRef]
45. Gaul, D.; Hertel, D.; Borken, W.; Matzner, E.; Leuschner, C. Effects of experimental drought on the fine root system of mature Norway spruce. *For. Ecol. Manag.* **2008**, *256*, 1151–1159. [CrossRef]
46. Mainiero, R.; Kazda, M. Depth-related fine root dynamics of Fagus sylvatica during exceptional drought. *For. Ecol. Manag.* **2006**, *237*, 135–142. [CrossRef]
47. Tierney, G.L.; Fahey, T.J.; Groffman, P.M.; Hardy, J.P.; Fitzhugh, R.D.; Driscoll, C.T.; Yavitt, J.B. Environmental control of fine root dynamics in a northern hardwood forest. *Glob. Chang. Biol.* **2003**, *9*, 670–679. [CrossRef]

48. Leuschner, C.; Backes, K.; Hertel, D.; Schipka, F.; Schmitt, U.; Terborg, O.; Runge, M. Drought responses at leaf, stem and fine root levels of competitive *Fagus sylvatica* L. and *Quercus petraea* (Matt.) Liebl. trees in dry and wet years. *For. Ecol. Manag.* **2001**, *149*, 33–46. [CrossRef]
49. Makkonen, K.; Helmisaari, H.-S. Seasonal and yearly variations of fine-root biomass and necromass in a Scots pine (*Pinus sylvestris* L.) stand. *For. Ecol. Manag.* **1998**, *102*, 283–290. [CrossRef]
50. Teskey, R.O.; Hinckley, T.M. Influence of temperature and water potential on root growth of white oak. *Physiol. Plant.* **1981**, *52*, 363–369. [CrossRef]
51. López, B.; Sabaté, S.; Gracia, C. Fine roots dynamics in a Mediterranean forest: Effects of drought and stem density. *Tree Physiol.* **1998**, *18*, 601–606. [CrossRef]
52. Leuschner, C.; Meier, I.C. The ecology of Central European tree species: Trait spectra, functional trade-offs, and ecological classification of adult trees. *Perspect. Plant Ecol. Evol. Syst.* **2018**, *33*, 89–103. [CrossRef]
53. Kubisch, P.; Hertel, D.; Leuschner, C. Do ectomycorrhizal and arbuscular mycorrhizal temperate tree species systematically differ in root order-related fine root morphology and biomass? *Front. Plant Sci.* **2015**, *6*, 64. [CrossRef]
54. Jacob, A.; Hertel, D.; Leuschner, C. Diversity and species identity effects on fine root productivity and turnover in a species-rich temperate broad-leaved forest. *Funct. Plant Biol.* **2014**, *41*, 678. [CrossRef]
55. Meinen, C.; Hertel, D.; Leuschner, C. Biomass and morphology of fine roots in temperate broad-leaved forests differing in tree species diversity: Is there evidence of below-ground overyielding? *Oecologia* **2009**, *161*, 99–111. [CrossRef]
56. Kaspar, F.; Müller-Westermeier, G.; Penda, E.; Mächel, H.; Zimmermann, K.; Kaiser-Weiss, A.; Deutschländer, T. Monitoring of climate change in Germany—Data, products and services of Germany's National Climate Data Centre. *Adv. Sci. Res.* **2013**, *10*, 99–106. [CrossRef]
57. Müller-Westermeier, G. *Numerisches Verfahren zu Erstellung Klimatologischer Karten*; Selbstverl. des Dt. Wetterdienstes: Offenbach am Main, Germany, 1995; ISBN 3881483063.
58. Maier, U.; Müller-Westermeier, G. *Verifikation Klimatologischer Rasterfelder*; Selbstverl. des Dt. Wetterdienstes: Offenbach am Main, Germany, 2010; ISBN 978-3-88148-450-3.
59. Löpmeier, F.J. Berechnung der Bodenfeuchte und Verdunstung mittels agrarmeteorologischer Modelle. *Zeitschrift f. Bewässerungswirtschaft* **1994**, *29*, 157–167.
60. Martonne, E.D. L'indice d'aridité. *Bulletin de L'Association de Géographes Français* **1926**, *3*, 3–5. [CrossRef]
61. Persson, H.Å. Root Dynamics in a Young Scots Pine Stand in Central Sweden. *Oikos* **1978**, *30*, 508. [CrossRef]
62. Bauhus, J.; Bartsch, N. Fine-root growth in beech (*Fagus sylvatica*) forest gaps. *Can. J. For. Res.* **1996**, *26*, 2153–2159. [CrossRef]
63. Lê, S.; Josse, J.; Husson, F. FactoMineR: An R Package for Multivariate Analysis. *J. Stat. Softw.* **2008**, *25*. [CrossRef]
64. Kassambara, A.; Mundt, F. Factoextra: Extract and Visualize the Results of Multivariate Data Analyses. 2017. Available online: https://CRAN.R-project.org/package=factoextra (accessed on 1 June 2019).
65. Bates, D.; Mächler, M.; Bolker, B.; Walker, S. Fitting Linear Mixed-Effects Models Using lme4. *J. Stat. Softw.* **2015**, *67*. [CrossRef]
66. Kuznetsova, A.; Brockhoff, P.; Christensen, R.H.B. lmerTest Package: Tests in Linear Mixed Effects Models. *J. Stat. Softw.* **2017**, *82*, 1–26. [CrossRef]
67. Nakagawa, S.; Schielzeth, H. A general and simple method for obtaining R2 from generalized linear mixed-effects models. *Methods Ecol. Evol.* **2013**, *4*, 133–142. [CrossRef]
68. Meier, I.C.; Knutzen, F.; Eder, L.M.; Müller-Haubold, H.; Goebel, M.-O.; Bachmann, J.; Hertel, D.; Leuschner, C. The Deep Root System of Fagus sylvatica on Sandy Soil: Structure and Variation Across a Precipitation Gradient. *Ecosystems* **2018**, *21*, 280–296. [CrossRef]
69. Joslin, J.D.; Wolfe, M.H.; Hanson, P.J. Effects of altered water regimes on forest root systems. *New Phytol.* **2000**, *147*, 117–129. [CrossRef]
70. Konôpka, B.; Lukac, M. Moderate drought alters biomass and depth distribution of fine roots in Norway spruce. *For. Path.* **2013**, *43*, 115–123. [CrossRef]
71. Persson, H.Å.; von Fircks, Y.; Majdi, H.; Nilsson, L.O. Root distribution in a Norway spruce (*Picea abies* (L.) Karst.) stand subjected to drought and ammonium-sulphate application. *Plant Soil* **1995**, *168*, 161–165. [CrossRef]
72. Schenk, H.J.; Jackson, R.B. The global biogeography of roots. *Ecol. Monogr.* **2002**, *72*, 311–328. [CrossRef]

73. Poorter, H.; Niklas, K.J.; Reich, P.B.; Oleksyn, J.; Poot, P.; Mommer, L. Biomass allocation to leaves, stems and roots: Meta-analyses of interspecific variation and environmental control. *New Phytol.* **2012**, *193*, 30–50. [CrossRef] [PubMed]
74. Kirfel, K.; Heinze, S.; Hertel, D.; Leuschner, C. Effects of bedrock type and soil chemistry on the fine roots of European beech—A study on the belowground plasticity of trees. *For. Ecol. Manag.* **2019**, *444*, 256–268. [CrossRef]
75. Leuschner, C.; Hertel, D.; Coners, H.; Büttner, V. Root competition between beech and oak: A hypothesis. *Oecologia* **2001**, *126*, 276–284. [CrossRef]
76. Rosengren, U.; Göransson, H.; Jönsson, U.; Stjernquist, I.; Thelin, G.; Wallander, H. Functional Biodiversity Aspects on the Nutrient Sustainability in Forests-Importance of Root Distribution. *J. Sustain. For.* **2006**, *21*, 77–100. [CrossRef]
77. Eissenstat, D.M.; McCormack, M.L.; Du, Q. Global change and root lifespan. In *Plant Roots: The Hidden Half*, 4th ed.; Eshel, A.B.T., Beeckmann, T., Eds.; Taylor and Francis Group/CRC Press: Boca Raton, FL, USA, 2013; pp. 27-1–27-13.
78. Ladefoged, K. Untersuchungen über die Periodizität im Ausbruch und Längenwachstum der Wurzeln bei Einigen unserer gewöhnlichsten Waldbäume. In *Dansk Resume*; AF Høst & Søn: Copenhagen, Denmark, 1939.
79. Liese, R.; Leuschner, C.; Meier, I.C. The effect of drought and season on root life span in temperate arbuscular mycorrhizal and ectomycorrhizal tree species. *J. Ecol.* **2019**, *34*, 187. [CrossRef]
80. Ostonen, I.; Lõhmus, K.; Helmisaari, H.-S.; Truu, J.; Meel, S. Fine root morphological adaptations in Scots pine, Norway spruce and silver birch along a latitudinal gradient in boreal forests. *Tree Physiol.* **2007**, *27*, 1627–1634. [CrossRef]
81. Lõhmus, K.; Truu, J.; Truu, M.; Kaar, E.; Ostonen, I.; Alama, S.; Kuznetsova, T.; Rosenvald, K.; Vares, A.; Uri, V.; et al. Black alder as a promising deciduous species for the reclaiming of oil shale mining areas. In *Brownfield Sites III—Prevention, Assessment, Rehabilitation and Development of Brownfield Sites*; Brebbia, C.A., Mander, Ü., Eds.; WIT: Southampton, UK, 2006; pp. 87–97, ISBN 1845640411.
82. Kunz, J.; Löffler, G.; Bauhus, J. Minor European broadleaved tree species are more drought-tolerant than Fagus sylvatica but not more tolerant than Quercus petraea. *For. Ecol. Manag.* **2018**, *414*, 15–27. [CrossRef]
83. Walentowski, H.; Falk, W.; Mette, T.; Kunz, J.; Bräuning, A.; Meinardus, C.; Zang, C.; Sutcliffe, L.M.E.; Leuschner, C. Assessing future suitability of tree species under climate change by multiple methods: A case study in southern Germany. *Ann. For. Res.* **2017**, *60*. [CrossRef]
84. Leuschner, C.; Wedde, P.; Lübbe, T. The relation between pressure–volume curve traits and stomatal regulation of water potential in five temperate broadleaf tree species. *Ann. For. Sci.* **2019**, *76*, 93. [CrossRef]
85. Köcher, P.; Gebauer, T.; Horna, V.; Leuschner, C. Leaf water status and stem xylem flux in relation to soil drought in five temperate broad-leaved tree species with contrasting water use strategies. *Ann. For. Sci.* **2009**, *66*, 101. [CrossRef]